Inorganic Chemistry
Article

Inorg. Chem. **2010**, *49*, 1687–1698 **1687**
DOI: 10.1021/ic902088x

Synthesis, Structures, Bonding, and Redox Chemistry of Ditungsten Butadiyne Complexes with W≡C—C≡W Backbones

Jibin Sun, Sarah E. Shaner, Marya K. Jones, Daniel C. O'Hanlon, Jeffrey S. Mugridge, and Michael D. Hopkins*

Department of Chemistry, The University of Chicago, 929 E. 57th Street, Chicago, Illinois 60637

Received October 21, 2009

Complexes of the form $XL_4W{\equiv}C{-}C{\equiv}WL_4X$ (L = 1/2 dmpe, 1/2 depe, $P(OMe)_3$; X = Cl, OTf) have been synthesized from $(Bu^tO)_3WCCW(OBu^t)_3$ in two steps via $Cl_3(dme)WCCW(dme)Cl_3$, which undergoes facile four-electron reduction in the presence of L. The compounds possess formal d^2-d^2 electron configurations. The molecular structures of $Cl(dmpe)_2WCCW(dmpe)_2Cl$ and $Cl\{P(OMe)_3\}_4WCCW\{P(OMe)_3\}_4Cl$ were determined by X-ray crystallography; bond distances within the backbone are consistent with a W≡C—C≡W canonical structure. Density-functional-theory calculations on $Cl(dmpe)_2WCCW(dmpe)_2Cl$ and the model compound $Cl(PH_3)_4WCCW(PH_3)_4Cl$, and on their monometallic analogs $W(CH)(dmpe)_2Cl$ and $W(CH)(PH_3)_4Cl$, indicate that the WCCW backbone is strongly π-conjugated; this is supported by the observation of low-energy $\pi \rightarrow \pi^*$ transitions for the compounds. The calculations predict that δ symmetry d_{xy}-derived orbitals should be (or lie near) the highest occupied molecular orbital. Consistent with this prediction, the electronic spectra of the compounds exhibit a band attributable to $d_{xy} \rightarrow \pi^*$ transition(s), as the lowest-energy feature and electrochemical studies demonstrate that they undergo sequential one-electron oxidations to produce $(d_{xy})^2-(d_{xy})^1$ and $(d_{xy})^1-(d_{xy})^1$ congeners. Due to the δ symmetry of the redox orbitals, the oxidized congeners maintain the W≡C—C≡W canonical structure of the parent d^2-d^2 compounds. The first and second oxidation potentials of $Cl(dmpe)_2WCCW(dmpe)_2Cl$ are separated by $\leq$0.4 V, corresponding to $K_{com} = 10^4-10^6$; the interaction between redox orbitals is largely electrostatic in origin and not the result of significant direct δ orbital overlap. The reaction between $Cl(dmpe)_2WCCW(dmpe)_2Cl$ and HCl (2 equiv) produces the d^0-d^0 dihydride ion $[Cl(H)(dmpe)_2WCCW(dmpe)_2(H)Cl]^{2+}$, which is formulated as maintaining the W≡C—C≡W backbone on the basis of its X-ray crystal structure and NMR spectra. This family of WCCW derivatives expands the relatively small class of M≡C—C≡M compounds and is distinctive among them because their ancillary ligands should allow incorporation of the L_4WCCWL_4 unit into interior positions of metalloyne oligomers and polymers.

Introduction

Within the broad class of metal-containing π-conjugated polymers and oligomers,[1] bimetallic complexes containing all-carbon linkers of type $L_nM(CC)_mML_n$ have been the focus of particular attention.[2−6] At a fundamental level, interest in these systems is driven by a set of questions common with those that motivate the effort to synthetically and theoretically model carbyne,[7] the elusive one-dimensional allotrope of carbon: these linear compounds are the simplest conjugated systems, and their bonding/property relationships will provide a conceptual framework for understanding and rationally designing more complex conjugated materials. Research by a number of groups over the past 15 years has resulted in the synthesis of metal-capped polyynes of impressive length ($m \rightarrow 14$)[8−11] and an understanding of the dependence on chain length of their molecular

*To whom correspondence should be addressed. E-mail: mhopkins@uchicago.edu.

(1) (a) Kingsborough, R. P.; Swager, T. M. *Prog. Inorg. Chem.* **1999**, *48*, 123. (b) Manners, I. *Synthetic Metal-Containing Polymers*; Wiley-VCH: Weinheim, Germany, 2004. (c) Williams, K. A.; Boydston, A. J.; Bielawski, C. W. *Chem. Soc. Rev.* **2007**, *36*, 729.
(2) Bruce, M. I.; Low, P. J. *Adv. Organomet. Chem.* **2004**, *50*, 179.
(3) (a) Szafert, S.; Gladysz, J. A. *Chem. Rev.* **2003**, *103*, 4175. (b) Szafert, S.; Gladysz, J. A. *Chem. Rev.* **2006**, *106*, PR1.
(4) Paul, F.; Lapinte, C. *Coord. Chem. Rev.* **1998**, *178*, 431.
(5) Venkatesan, K.; Blacque, O.; Berke, H. *Dalton Trans.* **2007**, 1091.
(6) Akita, M.; Koike, T. *Dalton Trans.* **2008**, 3523.
(7) (a) *Polyynes: Synthesis, Properties, and Applications*; Cataldo, F., Ed.; Taylor & Francis: Boca Raton, FL, 2005. (b) Chalifoux, W. A.; Tykwinski, R. R. *C. R. Chim.* **2009**, *12*, 341.
(8) Zheng, Q. L.; Bohling, J. C.; Peters, T. B.; Frisch, A. C.; Hampel, F.; Gladysz, J. A. *Chem.—Eur. J.* **2006**, *12*, 6486.
(9) Dembinski, R.; Bartik, T.; Bartik, B.; Jaeger, M.; Gladysz, J. A. *J. Am. Chem. Soc.* **2000**, *122*, 810.
(10) Mohr, W.; Stahl, J.; Hampel, F.; Gladysz, J. A. *Chem.—Eur. J.* **2003**, *9*, 3324.
(11) (a) Rigaut, S.; Perruchon, J.; Le Pichon, L.; Touchard, D.; Dixneuf, P. H. *J. Organomet. Chem.* **2003**, *670*, 37. (b) Antonova, A. B.; Bruce, M. I.; Elis, B. G.; Gaudio, M.; Humphrey, P. A.; Jevric, M.; Melino, G.; Nicholson, B. K.; Perkins, G. J.; Skelton, B. W.; Stapleton, B.; White, A. H.; Zaitseva, N. N. *Chem. Comm.* **2004**, 960. (c) Qi, H.; Gupta, A.; Noll, B. C.; Snider, G. L.; Lu, Y. H.; Lent, C.; Fehlner, T. P. *J. Am. Chem. Soc.* **2005**, *127*, 15218.

Published on Web 01/22/2010

Chart 1

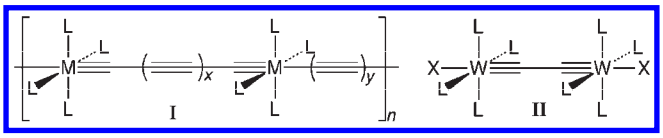

structures,[3] electronic structures,[12,13] linear[8−10] and nonlinear[14] optical properties, metal−metal redox[2,9,15] and magnetic[13] coupling, and photophysical properties.[16] This work has demonstrated that some electronic properties are changing with chain length even for the longest $L_nM(CC)_mML_n$ complexes, suggesting that the "carbyne limit" does not appear to have been reached.

There has been comparatively little experimental[17] or theoretical[18] effort directed toward $L_nM(CC)_mML_n$-containing compounds in which metal centers are incorporated into interior positions of polyyne chains in a manner that maintains the carbyne alternating bond-order structure, as exemplified by **I** in Chart 1. Such compounds would constitute an interesting complementary class to that of metal-capped $L_nM(CC)_mML_n$ complexes, both because the presence of periodic orthogonal ligands could stabilize longer oligomers and the interior metal centers would enable broader tuning of polyyne electronic structures and properties. One barrier to the potential development of this class of compounds is that **I** is derived from metal−alkylidyne-containing subunits of type $L_nM{\equiv}C(CC)_mC{\equiv}ML_n$, of which relatively few examples have been isolated.[19−23] Further, the ancillary ligands employed in these compounds (and, more generally, in previously studied $L_nM(CC)_mML_n$ compounds) do not provide opportunities for using them as interior building blocks for oligomers and polymers of type **I**.

Motivated by these considerations, we set out to prepare complexes of type **II** (Chart 1), the supporting ligands of which should allow insertion of the M≡C—C≡M unit into the interior of a polyyne rod or polymer. We report herein the synthesis, structures, bonding, and redox properties of d^2-d^2-configured compounds of the type XL_4WCCWL_4X (L = 1/2 dmpe (1,2-bis(dimethylphosphino)ethane), 1/2 depe (1,2-bis(diethylphosphino)ethane), $P(OMe)_3$; X = Cl, OTf). Density-functional theory calculations and electronic spectroscopy indicate that the electronic structures of these compounds are characterized by strong W≡C—C≡W π conjugation, and that δ symmetry metal-centered d orbitals lie near the highest occupied molecular orbital (HOMO). These latter redox-active orbitals allow electrochemical formation of d^2-d^1 and d^1-d^1 congeners and, via protonation, of the d^0-d^0 dihydride ion $[Cl(H)(dmpe)_2WCCW(dmpe)_2(H)Cl]^{2+}$; these congeners maintain the W≡C—C≡W canonical structure of the parent d^2-d^2 compounds. This family of complexes expands the relatively small class of M≡C—C≡M complexes and affords the opportunity to construct type-**I** materials that should possess broad redox properties yet robust carbyne-like molecular and electronic structures.

Experimental Section

General Procedures. All experiments were performed under a nitrogen atmosphere using standard Schlenk and glovebox techniques. HPLC-grade solvents, stored under nitrogen in stainless-steel cylinders, were purified by passing them under nitrogen pressure through an anaerobic, stainless-steel system consisting of either two 4.5 in. × 24 in. (1 gal) columns of activated A2 alumina (Et_2O, CH_2Cl_2, and THF) or one column of activated A2 alumina and one column of activated BASF R3-11 catalyst (toluene, pentane).[24] 1,2-Dimethoxyethane (DME) and C_6D_6 were purified by stirring over a NaK (1:2) alloy for 24 h, from which they were transferred under a vacuum. CD_2Cl_2 was dried by storage over P_2O_5, from which it was transferred under a vacuum. The compound $(Bu^tO)_3WCCW(OBu^t)_3$ was prepared according to the standard method.[19] Tetrabutylammonium hexafluorophosphate (electrochemical grade) was dried under a vacuum at 100 °C for 12 h. Ferrocene was recrystallized from 95% ethanol and then sublimed under a vacuum. All other reagents were obtained from commercial sources and used as received.

^1H, $^{13}C\{^1H\}$, $^{31}P\{^1H\}$, and $^{19}F\{^1H\}$ NMR spectra were recorded at room temperature using Bruker AF-500 or DRX 400 MHz NMR spectrometers. Chemical shifts were measured relative to solvent resonances (^1H, ^{13}C) or an external standard of 85% phosphoric acid (^{31}P) or $CFCl_3$ (^{19}F). Elemental analyses were performed by Midwest Microlab, LLC (Indianapolis, IN) or H. Kolbe Mikroanalytisches Laboratorium (Mülheim an der Ruhr, Germany). Electronic-absorption spectra were recorded using an Agilent Technologies 8453 UV−visible spectrophotometer of samples sealed in quartz cuvettes (1 cm or 1 mm path length). Extinction coefficients were calculated from plots of absorbance versus concentration of a combination of serially diluted and independently prepared samples.

Electrochemical Measurements. Electrochemical experiments were performed at room temperature under a nitrogen atmosphere in a glovebox using a Bioanalytical Systems 100 B/W Electrochemical Workstation and C3 cell stand. A three-electrode configuration was used, consisting of a Pt-disk working electrode (area = 0.2 cm^2), Pt-wire auxiliary electrode, and Ag-wire quasi-reference electrode. The electrodes were polished

(12) (a) Herrmann, C.; Neugebauer, J.; Gladysz, J. A.; Reiher, M. *Inorg. Chem.* **2005**, *44*, 6174. (b) Zhuravlev, F.; Gladysz, J. A. *Chem.—Eur. J.* **2004**, *10*, 6510.
(13) Paul, F.; Lapinte, C. In *Unusual Structures and Physical Properties in Organometallic Chemistry*; Gielen, M., Willem, R., Wrackmeyer, B., Eds.; John Wiley & Sons: West Sussex, U.K., 2002.
(14) Samoc, M.; Dalton, G. T.; Gladysz, J. A.; Zheng, Q.; Velkov, Y.; Agren, H.; Norman, P.; Humphrey, M. G. *Inorg. Chem.* **2008**, *47*, 9946.
(15) (a) Xu, G. L.; Zou, G.; Ni, Y. H.; DeRosa, M. C.; Crutchley, R. J.; Ren, T. *J. Am. Chem. Soc.* **2003**, *125*, 10057. (b) Low, P. J.; Roberts, R. L.; Cordiner, R. L.; Hartl, F. *J. Solid State Electrochem.* **2005**, *9*, 717. (c) Szafert, S.; Paul, F.; Meyer, W. E.; Gladysz, J. A.; Lapinte, C. *C. R. Chim.* **2008**, *11*, 693.
(16) (a) Che, C. M.; Chao, H. Y.; Miskowski, V. M.; Li, Y. Q.; Cheung, K. K. *J. Am. Chem. Soc.* **2001**, *123*, 4985. (b) Yam, V. W. W.; Wong, K. M. C. *Top. Curr. Chem.* **2005**, *257*, 1. (c) Yam, V. W. W.; Tao, C. H. In *Carbon-Rich Compounds*; Haley, M. M., Tykwinski, R. R., Eds.; Wiley-VCH: Weinheim, Germany, 2006; p 421. (d) de Quadras, L.; Shelton, A. H.; Kuhn, H.; Hampel, F.; Schanze, K. S.; Gladysz, J. A. *Organometallics* **2008**, *27*, 4979. (e) Farley, R. T.; Zheng, Q. L.; Gladysz, J. A.; Schanze, K. S. *Inorg. Chem.* **2008**, *47*, 2955.
(17) (a) Ren, T. *Organometallics* **2005**, *24*, 4854. (b) Manna, J.; Geib, S. J.; Hopkins, M. D. *J. Am. Chem. Soc.* **1992**, *114*, 9199.
(18) (a) Frapper, G.; Kertesz, M. *Inorg. Chem.* **1993**, *32*, 732. (b) Re, N.; Sgamellotti, A.; Floriani, C. *J. Chem. Soc., Dalton Trans.* **1998**, 2521.
(19) Listemann, M. L.; Schrock, R. R. *Organometallics* **1985**, *4*, 74.
(20) Caulton, K. G.; Cayton, R. H.; Chisholm, M. H.; Huffman, J. C.; Lobkovsky, E. B.; Xue, Z. *Organometallics* **1992**, *11*, 321.
(21) Frohnapfel, D. S.; Woodworth, B. E.; Thorp, H. H.; Templeton, J. L. *J. Phys. Chem. A* **1998**, *102*, 5665.
(22) Kheradmandan, S.; Venkatesan, K.; Blacque, O.; Schmalle, H. W.; Berke, H. *Chem.—Eur. J.* **2004**, *10*, 4872.
(23) (a) Gilbert, T. M.; Rogers, R. D. *J. Organomet. Chem.* **1991**, *421*, C1. (b) Gilbert, T. M.; Rogers, R. D. *Acta Crystallogr., Sect. C* **1993**, *49*, 677. (c) Woodworth, B. E.; White, P. S.; Templeton, J. L. *J. Am. Chem. Soc.* **1998**, *120*, 9028. (d) Dewhurst, R. D.; Hill, A. F.; Willis, A. C. *Organometallics* **2005**, *24*, 3043. (e) Colebatch, A. L.; Cordiner, R. L.; Hill, A. F.; Nguyen, K.; Shang, R.; Willis, A. C. *Organometallics* **2009**, *28*, 4394.
(24) Pangborn, A. B.; Giardello, M. A.; Grubbs, R. H.; Rosen, R. K.; Timmers, F. J. *Organometallics* **1996**, *15*, 1518.

prior to each experiment. Samples consisted of $0.3-5.0 \times 10^{-3}$ M analyte in THF or CH_2Cl_2 containing 0.3 M $[NBu_4][PF_6]$. Cyclic voltammetric experiments were conducted over a range of scan rates ($0.010-10$ V s^{-1}); values in parentheses associated with the electrode potentials indicate the range of $E_{1/2}$ values measured over scan rates of $0.010-1.00$ V s^{-1}. Ferrocene was used as an internal electrode-potential standard;[25] under the experimental conditions, the $FeCp_2^{0/+}$ couple exhibited $i_{pc}/i_{pa} \cong 1$ and $\Delta E_p = 0.09-0.27$ V. Peak currents were determined from scans that extended at least 0.30 V beyond the peak potentials before reaching the switching potential.

Computational Studies. Electronic-structure calculations were performed on the complexes $W(CH)(dmpe)_2Cl$ and $Cl(dmpe)_2WCCW(dmpe)_2Cl$ and model compounds $W(CH)(PH_3)_4Cl$ and $Cl(PH_3)_4WCCW(PH_3)_4Cl$ using density functional theory (DFT), as implemented in Gaussian 03.[26] The cc-pVTZ basis set[27] was used to describe the nonmetal atoms, and the SDB basis set and rECP combination,[28] supplemented by $2f+g$ functions,[29] was used for tungsten. Orbital energies were provided by calculations that employed the BP86 functional,[30,31] whereas the calculated molecular structure for $Cl(dmpe)_2WCCW(dmpe)_2Cl$ that agrees best with the crystal structure metrical data was provided by a calculation that employed the B3P86 functional.[30,32] B3P86 has been shown to give accurate geometries of third-row transition metal organometallic compounds.[33] Final optimized structures were obtained using tight convergence criteria and the ultrafine pruned (99,590) grid. Vibrational analyses were performed to ensure the absence of imaginary frequencies. The geometries of the compounds corresponded exactly or very closely to the maximum idealized symmetry ($W(CH)(PH_3)_4Cl$, C_{4v}; $Cl(PH_3)_4WCCW(PH_3)_4Cl$, D_{4h} (eclipsed) and D_{4d} (staggered); $W(CH)(dmpe)_2Cl$, C_2; and $Cl(dmpe)_2WCCW(dmpe)_2Cl$, C_2), with differences among symmetry-related bond distances and angles of the WCP_4Cl fragments being < 0.0001 Å and $< 0.01°$, respectively. The program AOMix[34] was used to calculate the atomic parentages of the molecular orbitals. Orbitals were rendered with Molekel.[35]

Cl_3(dme)WCCW(dme)Cl_3. To a solution of DME (7.74 g, 85.9 mmol) in toluene (10 mL) was added BCl_3 (17.5 mL, 1 M heptane solution, 17.5 mmol). The solution was cooled to −78 °C, and a solution of $(Bu^tO)_3WCCW(OBu^t)_3$ (2.38 g, 2.87 mmol) in toluene (150 mL) was slowly added with stirring. The reaction mixture was allowed to warm to room temperature. Over the course of 4 h, the color of the solution changed from pink to blue-green to colorless, and a brown-green precipitate formed. The precipitate was collected by filtration and washed with toluene (50 mL) and pentane (50 mL), which produced colorless filtrates. The solid was then washed with room-temperature DME (30 mL), which produced a dark-brown filtrate; the volatile components were removed from the remaining solid under a vacuum, leaving 2.43 g of material. This crude product was used in subsequent reactions without further purification. ^{1}H NMR (CD_2Cl_2, 400.13 MHz): δ 4.69 (s, 6 H, Me), 4.13 (t, 4 H, OCH_2CH_2), 3.87 (t, 4 H, OCH_2CH_2), 3.73 (s, 6 H, Me); resonances at 3.48 (s) and 3.33 (s) arising from 0.6 equiv of free DME are observed. Assuming no other impurities are present (none are observed by NMR), the mass of the product corresponds to ca. 100% yield. In various preparations, up to 3 equiv of free DME is contained in the product. Through trial and error, it was determined that assuming a yield of ca. 75% produced the highest yield of product in subsequent reduction reactions.

Cl(dmpe)$_2$WCCW(dmpe)$_2$Cl. To a brown-green room-temperature suspension of $Cl_3(dme)WCCW(dme)Cl_3$ (1.69 g, 2.15 mmol, assuming a 75% yield of $Cl_3(dme)WCCW(dme)Cl_3$) in THF (40 mL) was added dropwise with stirring DMPE (1.29 g, 8.59 mmol). Within 30 min, a rust orange precipitate formed. To this suspension was added Na/Hg (3.7 mL, 0.4 wt % Na, 8.69 mmol Na) over 5 min. The color of the reaction mixture changed from orange to red-brown within 1 h. After 5 h of vigorous stirring, the solution was dark red and precipitated NaCl was evident. The solution phase was decanted from the mercury layer, which was washed with THF (3×15 mL); the washings were combined with the crude product solution. Following the removal of solvent under a vacuum, the resulting red solid was extracted into toluene (50 mL) and the extract was filtered through Celite and reduced to dryness under a vacuum. The product was recrystallized from CH_2Cl_2/ether at −56 °C, which provided purple-red crystals (1.27 g, 42% yield based on $(Bu^tO)_3WCCW(OBu^t)_3$) suitable for X-ray diffraction studies. Lower product yields were observed if the mixture of $Cl_3(dme)WCCW(dme)Cl_3$ and DMPE was not allowed to stir for 20−30 min prior to the addition of the Na/Hg amalgam; if the Na/Hg amalgam was added quickly, or if the reaction time was < 2 h or > 36 h. ^{1}H NMR (CD_2Cl_2, 400.13 MHz): δ 1.72 (s, 24 H, Me), 1.52 (br, 8 H, PCH_2CH_2P), 1.44 (br sh, 8 H, PCH_2CH_2P), 1.41 (s, 24 H, Me). $^{31}P\{^1H\}$ NMR (CD_2Cl_2, 161.98 MHz): δ 24.7 (s with br satellites, $^1J_{PW} = 280$ Hz). ^{1}H NMR (C_6D_6, 500.13 MHz): δ 1.61 (s, 24 H, Me), 1.54 (br sh, 8 H, PCH_2CH_2P) and 1.51 (s, 24 H, Me), 1.33 (br, 8 H, PCH_2CH_2P). $^{13}C\{^1H\}$ NMR (C_6D_6, 125.77 MHz): δ 274.4 (W≡C), 33.7, 21.8, 17.3. $^{31}P\{^1H\}$ NMR (C_6D_6, 202.46 MHz): δ 24.4 (s with br satellites, $^1J_{PW} = 280$ Hz). Anal. Calcd (found) for $C_{26}Cl_2H_{64}P_8W_2$: C, 29.37 (29.43); H, 6.07 (5.98).

Cl(depe)$_2$WCCW(depe)$_2$Cl. This compound was prepared analogously to $Cl(dmpe)_2WCCW(dmpe)_2Cl$ and isolated in 27% yield (based on $(Bu^tO)_3WCCW(OBu^t)_3$) after recrystallization from toluene at −56 °C. ^{1}H NMR (THF-d_8, 500.13 MHz): δ 2.13, 2.00, 1.91, 1.77, 1.59, 1.42, 1.27 (sh), 1.19 (sh), 1.14 (m, PCH_2CH_3), 1.07 (m, PCH_2CH_3); accurate integration precluded by overlapping, broad resonances. $^{31}P\{^1H\}$ NMR (C_6D_6, 161.98 MHz): δ 40.0 (s, $^1J_{PW} = 275$ Hz). The thermal instability of this compound precluded obtaining an acceptable elemental analysis.

Cl{P(OMe)$_3$}$_4$WCCW{P(OMe)$_3$}$_4$Cl. This compound (brown in color) was prepared analogously to $Cl(dmpe)_2WCCW(dmpe)_2Cl$ and isolated in 28% yield (based on $(Bu^tO)_3WCCW(OBu^t)_3$) after recrystallization from toluene/pentane at −40 °C.

(25) Gritzner, G.; Kuta, J. *Pure Appl. Chem.* **1984**, *56*, 461.
(26) Frisch, M. J.; Trucks, G. W.; Schlegel, H. B.; Scuseria, G. E.; Robb, M. A.; Cheeseman, J. R.; Montgomery, J. A.; Vreven, T.; Kudin, K. N.; Burant, J. C.; Millam, J. M.; Iyengar, S. S.; Tomasi, J.; Barone, V.; Mennucci, B.; Cossi, M.; Scalmani, G.; Rega, N.; Petersson, G. A.; Nakatsuji, H.; Hada, M.; Ehara, M.; Toyota, K.; Fukuda, R.; Hasegawa, J.; Ishida, M.; Nakajima, T.; Honda, Y.; Kitao, O.; Nakai, H.; Klene, M.; Li, X.; Knox, J. E.; Hratchian, H. P.; Cross, J. B.; Bakken, V.; Adamo, C.; Jaramillo, J.; Gomperts, R.; Stratmann, R. E.; Yazyev, O.; Austin, A. J.; Cammi, R.; Pomelli, C.; Ochterski, J. W.; Ayala, P. Y.; Morokuma, K.; Voth, G. A.; Salvador, P.; Dannenberg, J. J.; Zakrzewski, V. G.; Dapprich, S.; Daniels, A. D.; Strain, M. C.; Farkas, O.; Malick, D. K.; Rabuck, A. D.; Raghavachari, K.; Foresman, J. B.; Ortiz, J. V.; Cui, Q.; Baboul, A. G.; Clifford, S.; Cioslowski, J.; Stefanov, B. B.; Liu, G.; Liashenko, A.; Piskorz, P.; Komaromi, I.; Martin, R. L.; Fox, D. J.; Keith, T.; Laham, A.; Peng, C. Y.; Nanayakkara, A.; Challacombe, M.; Gill, P. M. W.; Johnson, B.; Chen, W.; Wong, M. W.; Gonzalez, C.; Pople, J. A. *Gaussian 03*, revision E.01; Gaussian, Inc.: Wallingford, CT, 2004.
(27) Kendall, R. A.; Dunning, J. T. H.; Harrison, R. J. *J. Chem. Phys.* **1992**, *96*, 6796.
(28) Andrae, D.; Häussermann, U.; Dolg, M.; Stoll, H.; Preuss, H. *Theor. Chim. Acta* **1990**, *77*, 123.
(29) Martin, J. M. L.; Sundermann, A. *J. Chem. Phys.* **2001**, *114*, 3408.
(30) Perdew, J. P. *Phys. Rev. B* **1986**, *33*, 8822.
(31) Becke, A. D. *Phys. Rev. A* **1988**, *38*, 3098.
(32) Becke, A. D. *J. Chem. Phys.* **1993**, *98*, 5648.
(33) Bühl, M.; Reimann, C.; Pantazis, D. A.; Bredow, T.; Neese, F. *J. Chem. Theory Comput.* **2008**, *4*, 1449.
(34) Gorelsky, S. I. *AOMix 6.36*; Department of Chemistry, York University: Toronto, ON, 1997. http://www.sg-chem.net (accessed Jan 2010).
(35) Flükiger, P.; Lüthi, H. P.; Portmann, S.; Weber, J. *MOLEKEL 4.3*; Swiss Center for Scientific Computing: Manno, Switzerland.

Table 1. Crystal Data and Data Collection and Refinement Parameters for $Cl(dmpe)_2WCCW(dmpe)_2Cl\cdot 3CH_2Cl_2$ (**1**), $Cl\{P(OMe)_3\}_4WCCW\{P(OMe)_3\}_4Cl$ (**2**), and $[Cl(H)(dmpe)_2WCCW(dmpe)_2(H)Cl]Cl_2\cdot 2CH_3CN$ (**3**)

parameter	1	2	3
formula	$C_{29}H_{70}Cl_8P_8W_2$	$C_{26}H_{72}Cl_2O_{24}P_8W_2$	$C_{30}H_{72}Cl_4N_2P_8W_2$
space group	$P2_12_12_1$	$P2_1/c$	$C2/c$
a, Å	15.733(3)	10.984(6)	29.849(6)
b, Å	16.348(3)	19.242(10)	10.400(2)
c, Å	19.759(4)	19.242(10)	18.048(4)
β, deg	90	113.442(17)	121.12(3)
V, Å^3	5082.2(16)	5221(4)	4796.3(17)
Z	4	4	4
λ, Å	0.71073	0.71073	0.71073
ρ_{calcd}, g/cm^3	1.711	1.851	1.684
μ, mm^{-1}	5.216	4.823	5.306
T, K	100	100	100
R1, wR2 [$I > 2\sigma(I)$]	0.0375, 0.0840	0.1391, 0.3012	0.0462, 0.0837
R1, wR2 (all data)	0.0404, 0.0855	0.1441, 0.3037	0.0535, 0.0856

^{1}H NMR (500.13 MHz, C_6D_6): δ 3.79 (s, OCH_3). ^{13}C NMR (125.77 MHz, C_6D_6): δ 52.6 (s, OMe); WC not observed. ^{31}P NMR (202.47 MHz, C_6D_6): δ 150.6 (s, $^1J_{PW}$ = 436 Hz). The thermal instability of this compound precluded obtaining an acceptable elemental analysis.

(TfO)(dmpe)$_2$WCCW(dmpe)$_2$(OTf). To a stirred, room-temperature solution of $Cl(dmpe)_2WCCW(dmpe)_2Cl$ (1.16 g, 1.09 mmol) in toluene (40 mL) was added $SiMe_3(OTf)$ (0.50 g, 2.25 mmol). The progress of the reaction was monitored by ^{31}P NMR spectroscopy. After 1 h, the red-purple reaction mixture was decanted from a small amount of dark, toluene-insoluble precipitate, and the volatile components were removed under a vacuum. The remaining red-purple solid (1.08 g, 77% yield) exhibited ^{31}P and ^{1}H NMR spectra consistent with the expected product and without evidence of impurities; it was used without further purification. ^{1}H NMR (C_6D_6, 500.13 MHz): δ 1.58 (br, 8 H, PCH_2CH_2P), 1.48 (s, 24 H, Me), 1.39 (s, 24 H, Me), 1.20 (br, 8 H, PCH_2CH_2P). ^{31}P{^{1}H} NMR (C_6D_6, 202.46 MHz): δ 31.5 (s, $^1J_{PW}$ = 282 Hz). ^{19}F{^{1}H} NMR (C_6D_6, 470.56 MHz), δ −77.4 (s). APCI-MS (toluene/CH_3CN): m/z 1182.1 (M^+ − OTf + CH_3CN).

[Cl(H)(dmpe)$_2$WCCW(dmpe)$_2$(H)Cl]Cl$_2$. To a stirred solution of $Cl(dmpe)_2WCCW(dmpe)_2Cl$ (0.201 g, 0.189 mmol) in THF (30 mL) at −78 °C was added HCl (0.40 mL, 1 M solution in diethyl ether, 0.40 mmol). The reaction mixture changed in color from purple-red to brown, and a light-colored precipitate was observed immediately. After 1 h, the volatile components were removed under a vacuum, and the remaining tan solid was washed with toluene (3 × 15 mL). Precipitation of this material from CH_2Cl_2 layered with Et_2O (1:1) at −50 °C provided the product as a pale yellow solid (0.175 g, 81% yield). Microcrystals grown by vapor diffusion of diethyl ether into an acetonitrile solution of the product appear light brown in color. ^{1}H NMR (CD_2Cl_2, 400.13 MHz): 2.58 (quintet, 2 H, J_{HP} = 40.4 Hz, WH), 2.15 (d with sh, 40 H, PCH_2CH_2P, Me), 1.75 (d, 24 H, Me). ^{13}C{^{1}H} NMR (CD_2Cl_2, 125.77 MHz): δ 29.5, 20.9, 14.6 (br); WC not observed. ^{31}P{^{1}H} NMR (CD_2Cl_2, 161.98 MHz): δ 30 (v br). ESI-MS (CH_3CN): m/z 532.0 (M^{2+}).

Single-Crystal X-Ray Diffraction Studies. Single-crystal X-ray diffraction data were obtained using a Bruker AXS SMART APEX diffractometer. Crystals were coated with Fluorolube oil and examined by optical microscopy; those of a suitable size and an equidimensional shape that exhibited good extinction under polarized light were mounted to a glass fiber and affixed to the goniometer in the path of a stream of cold nitrogen (100 K). Rotation and still images showed the diffractions to be sharp. Frames separated in reciprocal space were obtained and provided an orientation matrix and initial cell parameters. Final cell parameters were obtained from the full data set. A "full sphere" of data was obtained that included all diffractions up to a resolution of 0.84 Å (for $Cl(dmpe)_2WCCW(dmpe)_2Cl$ and $[Cl(dmpe)_2(H)WCCW(H)(dmpe)_2Cl]Cl_2$) or 0.75 Å ($Cl\{P(OMe)_3\}_4WCCW\{P(OMe)_3\}_4Cl$) using 0.3° steps in ω, with integration times of 20 and 15 s/frame, respectively. Integrated intensities were obtained using the program SAINT (v. 6.02), and corrections for absorption were made using SADABS (v. 2.03) on the basis of redundant reflections. Structure solution was accomplished using the program SHELXTL (v. 5.1). Crystal data and data collection and refinement parameters are set out in Table 1. The structure of $[Cl(dmpe)_2(H)WCCW(H)(dmpe)_2Cl]Cl_2$ was solved without difficulty; complications with the structures of $Cl(dmpe)_2WCCW(dmpe)_2Cl$ and $Cl\{P(OMe)_3\}_4WCCW\{P(OMe)_3\}_4Cl$ are described below.

Structure of Cl(dmpe)$_2$WCCW(dmpe)$_2$Cl. Patterson methods were used to locate the W and some P atoms. Repeated difference Fourier maps allowed recognition of all W, P, Cl, and C atoms. It became clear that the arrangement of the phosphorus nuclei around W(1) was ordered (e.g., normal intra- and interligand P−W(1)−P angles of 81° and 99°, respectively, were observed) but that the dmpe ligands about W(2) were rotationally disordered with respect to the central WCCW axis, as evidenced by the fact that the cis P−W(2)−P angles appear to be ca. 90°. The disorder about W(2) could be modeled with four PCCP linkages of approximately 1/2 occupancy for the two carbons of each bridge. The two terminal C atoms on each P also exhibited disorder resulting from the structural constraints of the PCCP bridges on either side. The bridging C atoms of the dmpe ligands about W(2) were refined isotropically, while the terminal C atoms on each P were refined anisotropically (but showed elongated displacements due to the disorder). All atoms about W(1) were refined anisotropically. The thermal ellipsoids for C(9) and C(10) and the C(9)−C(10) distance are consistent with unresolved disorder between two skew-boat conformations of the dmpe backbone.

Structure of Cl{P(OMe)$_3$}$_4$WCCW{P(OMe)$_3$}$_4$Cl. The space group was determined as $P2_1/c$ on the basis of systematic absences and intensity statistics. A set of weak diffractions suggested a larger cell, but solution in this larger cell was unsuccessful. For the smaller cell, direct methods were used to locate the W and P atoms from the E map. Repeated difference Fourier maps allowed recognition of all of the C and O atoms. It became clear that one W and associated P, O, and C atoms behaved well, while the other W atom had four P atoms with occupancies of 0.71 and four other P atoms with occupancies of 0.29. For the major-occupancy $P(OMe)_3$ ligands, the P, O, and C atoms were included in the refinement, while for the minor-occupancy counterparts only the P atoms were included. Final refinement was anisotropic for all non-H atoms and isotropic-riding for H atoms. Two nonpositive-definite C atoms are present. As a result of these problems (reflected in the large R values), the structure is taken to convey only the connectivity of the $W_2(PO_3)_8Cl_2$ core; metrical data[36] are presumed to be unsuitable for quantitative analysis.

(36) See the Supporting Information.

Scheme 1. Synthesis of d^0-d^0 and d^2-d^2 L_nWCCWL_n Complexes

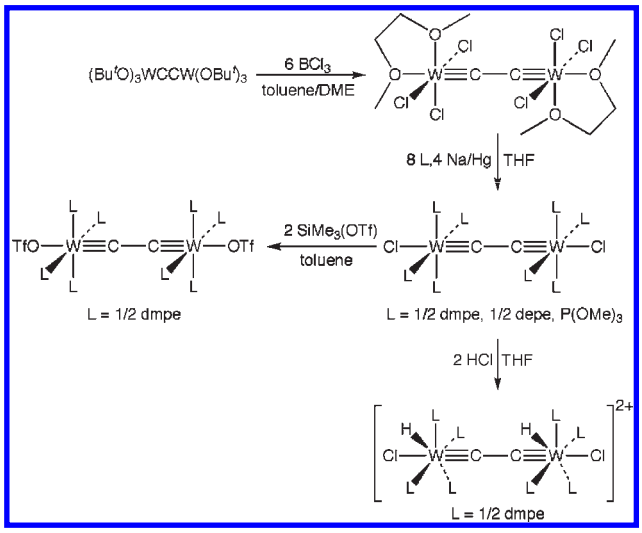

Results and Discussion

Synthesis and Characterization of d^0-d^0 and d^2-d^2 L_nWCCWL_n Complexes. The entry point to the new WCCW-containing compounds is the previously reported d^0-d^0 complex $(Bu^tO)_3WCCW(OBu^t)_3$, which is easily prepared in >90% yield via the triple-bond metathesis reaction between $W_2(OBu^t)_6$ and an internal diyne.[19] The synthetic transformations that provide the derivatives of this compound are summarized in Scheme 1. The reaction between $(Bu^tO)_3WCCW(OBu^t)_3$ and excess BCl_3 and 1,2-dimethoxyethane (DME) results in replacement of the *t*-butoxide ligands by chloride and ligation of DME, providing brownish-green d^0-d^0 $Cl_3(dme)WCCW(dme)Cl_3$. This transformation is analogous to those reported previously for the preparation of monometallic $W(CR)(dme)X_3$ compounds from $W(CR)(OBu^t)_3$ precursors,[37] with a difference being that in the present case the synthesis proceeds more cleanly if $(Bu^tO)_3WCCW(OBu^t)_3$ is added slowly to BCl_3 and DME rather than added quickly or in the reverse order (as done for $W(CR)(dme)X_3$ compounds). We speculate that this order and rate of addition minimizes the buildup of mixed-ligand $W_2C_2(OBu^t)_{6-n}Cl_n$ intermediates, which might precipitate prior to formation of the final product. It is important to minimize impurities in the crude product of $Cl_3(dme)WCCW(dme)Cl_3$ because its limited solubility in common organic solvents makes recrystallization of the compound difficult. Fortunately, these impurities do not appear to interfere with subsequent reduction reactions of this complex.

Complexes of the general form ClL_4WCCWL_4Cl, which possess formal d^2-d^2 electron configurations, are prepared via the four-electron reduction of $Cl_3(dme)WCCW(dme)Cl_3$ by Na/Hg amalgam in the presence of phosphorus ligands (L = 1/2 dmpe, 1/2 depe, $P(OMe)_3$; Scheme 1). This reaction is analogous to that for monometallic $W(CR)(dme)Cl_3$ complexes.[38,39] The stability of the ClL_4WCCWL_4Cl products is a strong function of the L ligands. The red-purple dmpe derivative $Cl(dmpe)_2WCCW(dmpe)_2Cl$ is stable as a solid at room temperature and can be stored under nitrogen for over one year at −33 °C without decomposition. The formulation of the compound was established by X-ray crystallography (vide infra); ^1H, ^{13}C, and ^{31}P NMR spectroscopy; and elemental analysis. The ^{13}C NMR resonance at δ 274 attributed to the WCCW nuclei is diagnostic of a $W(\equiv CR)(PR'_3)_4X$-containing complex.[39,40] The compounds $Cl(depe)_2WCCW(depe)_2Cl$ (red-purple in color) and $Cl\{P(OMe)_3\}_4WCCW\{P(OMe)_3\}_4Cl$ (brown) are less stable. Solid samples of $Cl(depe)_2WCCW(depe)_2Cl$ stored under an inert atmosphere at −33 °C exhibited decomposition within one week of their preparation, as indicated by the presence of free DEPE in the ^{31}P NMR spectrum, while solid $Cl\{P(OMe)_3\}_4WCCW\{P(OMe)_3\}_4Cl$ showed decomposition within one month. The depe and $P(OMe)_3$ derivatives decompose more quickly in solution. The instability of these compounds hindered their characterization, although they appear by the available measures to be analogous to $Cl(dmpe)_2WCCW(dmpe)_2Cl$. The compounds are soluble in toluene, THF, and CH_2Cl_2. The instability of $Cl(depe)_2WCCW(depe)_2Cl$ is undoubtedly the result of steric factors, as suggested by the structure of $Cl(dmpe)_2WCCW(dmpe)_2Cl$ (vide infra), whereas that of $Cl\{P(OMe)_3\}_4WCCW\{P(OMe)_3\}_4Cl$ may arise from the lability of $P(OMe)_3$, since for $W(CPh)\{P(OMe)_3\}_4Cl$ these ligands are reported to undergo facile substitution reactions.[41]

The reaction between $Cl(dmpe)_2WCCW(dmpe)_2Cl$ and $SiMe_3(OTf)$ (2 equiv) in toluene gave the light-purple, air-sensitive complex $(TfO)(dmpe)_2WCCW(dmpe)_2(OTf)$ in 90% yield. Triflate derivatives of mononuclear d^2 tungsten−alkylidyne complexes, prepared analogously,[42] have been reported to be substantially more reactive toward axial ligand substitution than the chloride complexes. The OTf-substitution reactions of $(TfO)(dmpe)_2WCCW(dmpe)_2(OTf)$ will be reported separately.

Treatment of d^2-d^2 $Cl(dmpe)_2WCCW(dmpe)_2Cl$ with 2 equiv of HCl provides the pale-yellow d^0-d^0 dihydride compound $[Cl(H)(dmpe)_2WCCW(dmpe)_2(H)Cl]Cl_2$. This reaction is analogous to that reported for monometallic $W(CR)(PR'_3)_4$ complexes (R = H, Bu^t; PR'_3 = PMe_3, 1/2 dmpe).[39,43] The cation is formulated as an alkylidyne hydride compound with a pseudo-pentagonal-bipyramidal structure about each metal center, rather than an alkylidene complex of the form $[Cl(dmpe)_2W{=}CH{-}CH{=}W(dmpe)_2Cl]^{2+}$, on the basis of the X-ray crystal structure of the salt (vide infra) and the ^1H NMR spectrum, which exhibits a characteristic hydride resonance (δ 2.58, quintet). The ^{31}P NMR spectrum of the compound exhibits a very broad singlet at room temperature, which separates into two multiplets at $T <$ 260 K. Similar ^{31}P NMR spectra have been reported by Schrock et al. for monometallic compounds of the form $[M(CR)(H)(dmpe)_2X]^{n+}$ (M = Ta, $n = 0$; M = W, $n = 1$;

(37) (a) Stevenson, M. A.; Hopkins, M. D. *Organometallics* **1997**, *16*, 3572. (b) Sun, J.; Simpson, C. K.; Hopkins, M. D. *Inorg. Synth.* In press.
(38) Mayr, A.; Asaro, M. F.; Kjelsberg, M. A.; Lee, K. S.; Van Engen, D. *Organometallics* **1987**, *6*, 432.
(39) Holmes, S. J.; Clark, D. N.; Turner, H. W.; Schrock, R. R. *J. Am. Chem. Soc.* **1982**, *104*, 6322.
(40) John, K. D.; Hopkins, M. D. *Chem. Comm.* **1999**, 589.
(41) Mayr, A.; Dorries, A. M.; McDermott, G. A.; van Engen, D. *Organometallics* **1986**, *5*, 1504.
(42) Holmes, S. J.; Schrock, R. R.; Churchill, M. R.; Wasserman, H. J. *Organometallics* **1984**, *3*, 476.
(43) Holmes, S. J.; Schrock, R. R. *J. Am. Chem. Soc.* **1981**, *103*, 4599.

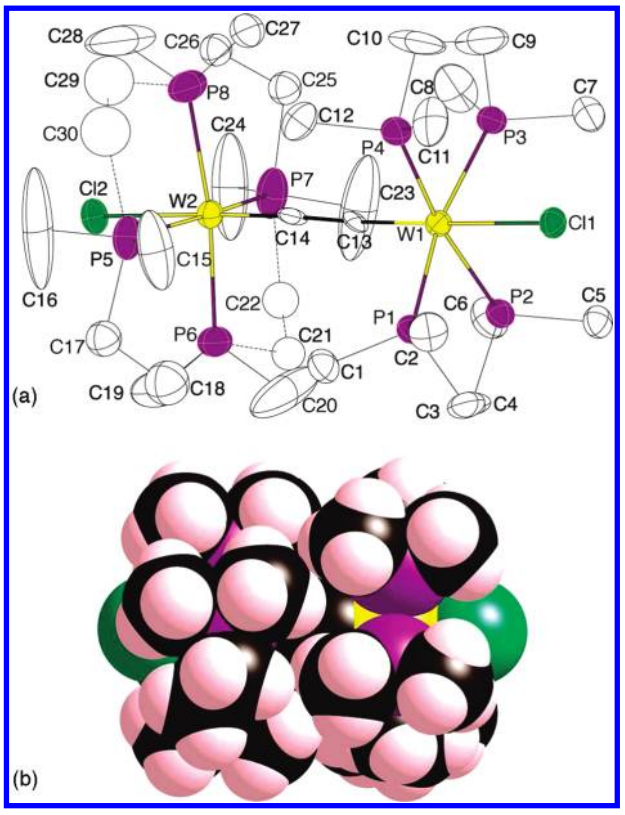

Figure 1. Molecular structure of $Cl(dmpe)_2WCCW(dmpe)_2Cl$: (a) Thermal-ellipsoid representation drawn at the 50% probability level, with hydrogen atoms omitted for clarity and the disordered orientation shown with dotted bonds; (b) space-filling model.

X = Cl, I, OTf)[43,44] and interpreted as indicating a fluxional structure with intermediacy of an alkylidene ligand; the details for the present compound are more complicated and will be described elsewhere.

Single-Crystal X-Ray Diffraction Studies. The molecular structures of $Cl(dmpe)_2WCCW(dmpe)_2Cl$, $Cl\{P(OMe)_3\}_4WCCW\{P(OMe)_3\}_4Cl$, and $[Cl(H)(dmpe)_2WCCW(dmpe)_2(H)Cl]Cl_2$ were determined by X-ray crystallography. Thermal ellipsoid representations of the structures are shown in Figures 1−3, and important bond distances and angles are set out in Table 2. As described below, a common feature of all compounds is that they exhibit bond distances consistent with a W≡C—C≡W structure.

The structure of d^2−d^2 $Cl(dmpe)_2WCCW(dmpe)_2Cl$ (Figure 1a) exhibits the expected pseudo-octahedral coordination at the tungsten centers, with linear Cl—W≡C—C≡W—Cl backbones (∠Cl—W≡C, ∠W≡C—C ≥ 175°) and equatorial phosphine ligands. The average W≡C distance (1.844[6] Å) is similar to that of $(Bu^tO)_3WCCW(O^tBu)_3$ (1.819(16) Å),[20] the only other structurally characterized W≡C—C≡W-containing compound, and to other d^2 $W(CR)(PR_3)_4Cl$ compounds ($W(CPh)(dppe)_2Cl$, 1.833(5);[45] $W(CH)(dmpe)_2Cl$, 1.797(10)).[46] Correspondingly, the C—C distance (1.410(9) Å) is within 2.58σ of

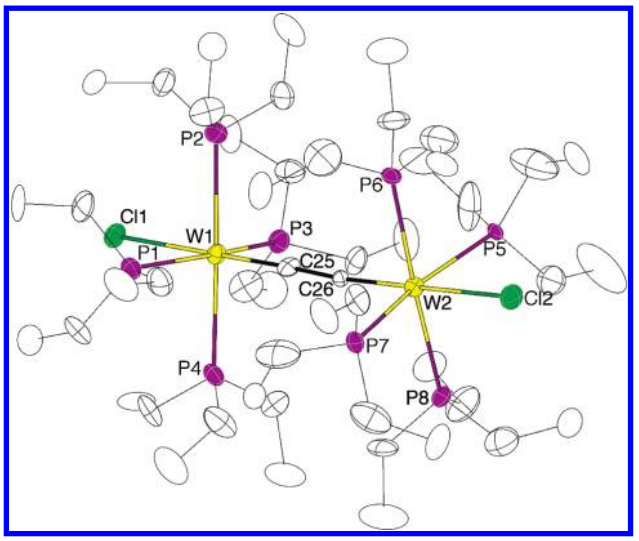

Figure 2. Thermal-ellipsoid representation of $Cl\{P(OMe)_3\}_4WCCW\{P(OMe)_3\}_4Cl$ drawn at the 40% probability level, with hydrogen atoms omitted for clarity.

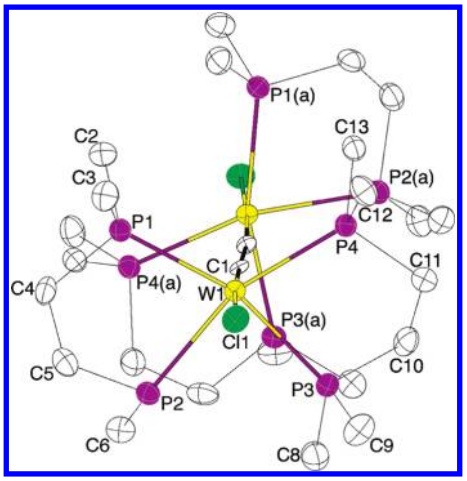

Figure 3. Thermal-ellipsoid representation of the dication of $[Cl(dmpe)_2(H)WCCW(H)(dmpe)_2Cl]Cl_2$ drawn at the 50% probability level, with hydrogen atoms omitted for clarity.

that for an sp-hybridized C—C single bond (1.37−1.38 Å),[3] and substantially longer than that expected for a metal−acetylide complex (i.e., WC≡CW).[47] These data suggest that the backbone of $Cl(dmpe)_2WCCW(dmpe)_2Cl$ is well described by the W≡C—C≡W canonical structure. As typical for a metal−alkylidyne complex, the W—Cl bonds are very long due to the strong trans influence of the M≡C bond. The structure of $Cl\{P(OMe)_3\}_4WCCW\{P(OMe)_3\}_4Cl$ (Figure 2) is of low quality but clearly is qualitatively similar to that of $Cl(dmpe)_2WCCW(dmpe)_2Cl$. Both compounds possess nonbonded W···W distances of ca. 5.1 Å.

A space-filling model of $Cl(dmpe)_2WCCW(dmpe)_2Cl$, shown in Figure 1b, illustrates the close contact between its $W(dmpe)_2$ fragments. Although the van der Waals surfaces of the two halves appear to be interdigitated, the ^1H, ^{13}C, and ^{31}P NMR resonances of the compound are consistent with free rotation about the WCCW axis in solution at room temperature. The crowded structure of

(44) Churchill, M. R.; Wasserman, H. J.; Turner, H. W.; Schrock, R. R. *J. Am. Chem. Soc.* **1982**, *104*, 1710.
(45) Cohen, B. W.; Simpson, C. K.; Hopkins, M. D. Manuscript in preparation.
(46) Manna, J.; Mlinar, L. A.; Kuk, R. J.; Dallinger, R. F.; Geib, S. J.; Hopkins, M. D. In *Transition Metal Carbyne Complexes*; Kreissl, F. R., Ed.; Kluwer Academic Publishers: Dordrecht, The Netherlands, 1992; p 75.
(47) Manna, J.; John, K. D.; Hopkins, M. D. *Adv. Organomet. Chem.* **1995**, *38*, 79.

Table 2. Bond Distances (Å) and Angles (deg) for $Cl(dmpe)_2WCCW(dmpe)_2Cl$ (**1**) and $[Cl(H)(dmpe)_2WCCW(dmpe)_2(H)Cl]Cl_2$ (**3**)

nuclei	**1**	**3**
W≡C	1.848 (6)	1.852 (7)
	1.839 (6)	
WC—CW	1.410 (9)	1.375 (13)
W···W	5.097	5.079
W—P(1)	2.439(2)[a]	2.4843(19)
W—P(2)	2.442(2)[a]	2.546(2)
W—P(3)	2.422(2)[a]	2.5166(19)
W—P(4)	2.4331(19)[a]	2.4594(19)
$W—P_{avg}$	2.434[2][a]	2.472[2], 2.531[2]
W—Cl	2.6028 (17)	2.5564 (17)
	2.5938 (18)	
W≡C—C	176.9 (5)	174.5 (6)
	177.0 (5)	
Cl—W≡C	177.8 (2)	176.64 (19)
	178.03 (19)	
P(1)—W—P(2)	80.19(7)[a]	77.89(6)
P(2)—W—P(3)	97.06(7)[a]	84.69(6)
P(3)—W—P(4)	80.38(7)[a]	77.04(6)
P(4)—W—P(1)	100.16(8)[a]	119.59(6)

[a] Datum for ordered fragment.

$Cl(dmpe)_2WCCW(dmpe)_2Cl$ undoubtedly accounts for the instability of $Cl(depe)_2WCCW(depe)_2Cl$, whose phosphine ligands are more sterically demanding.

The structure of d^0-d^0 $[Cl(H)(dmpe)_2WCCW(dmpe)_2(H)Cl]Cl_2$, shown in Figure 3, exhibits a pseudo-pentagonal-bipyramidal geometry about each metal center and a W≡C—C≡W backbone: the W≡C distance (1.852(7) Å, Table 2) is nearly identical to that for $Cl(dmpe)_2WCCW(dmpe)_2Cl$ (1.844(6) Å), and the WC—CW distance (1.375(13) Å) is consistent with an sp-hybridized WC—CW bond. These data exclude the presence in the solid state of an alkylidene linkage of the form W=CH—CH=W, which would result from protonation of the α carbon atoms. The hydride ligands are not observed in the crystal structure but are inferred to lie near the equatorial plane on the basis of the similarity between the geometry of the $M(dmpe)_2$ unit and that of $Ta(CBu^t)(H)(dmpe)_2(ClAlMe_3)$, for which an equatorial hydride ligand (∠(CTaH) = 100.4(16)°) was located in the crystal structure.[44] Specifically, the $W(dmpe)_2$ unit exhibits two markedly different interligand P—W—P bond angles (119.59(6) and 84.69(6)°), with the W—P bonds that form the compressed angle being 0.07 Å longer than those that define the larger angle. These values are very similar to those for the tantalum complex (∠(PTaP) = 123.02(6)° and 85.53(6)°, Δ*d*(Ta—P) = 0.09 Å).[44] The W—Cl bond distance of $[Cl(H)(dmpe)_2WCCW(dmpe)_2(H)Cl]Cl_2$ (2.5564(17) Å) is 0.04 Å shorter than that for $Cl(dmpe)_2WCCW(dmpe)_2Cl$, presumably because the smaller ionic radius of W^{VI} than that of W^{IV} counteracts the expected bond-radius increase associated with expanding the tungsten coordination number from six to seven.

Electronic Structures of d^2-d^2 ClL_4WCCWL_4Cl Complexes. The electronic structures of $Cl(dmpe)_2WCCW(dmpe)_2Cl$ and the idealized model compound $Cl(PH_3)_4WCCW(PH_3)_4Cl$, and those of their monometallic analogs $W(CH)(dmpe)_2Cl$ and $W(CH)(PH_3)_4Cl$,[48] were investigated using density functional theory in order to provide a basis for interpreting the physical properties of d^2-d^2 XL_4WCCWL_4X complexes and to probe the nature of π conjugation within the W≡C—C≡W unit. The model complexes are the basis for this discussion because their high symmetry (D_{4h} for $Cl(PH_3)_4WCCW(PH_3)_4Cl$, C_{4v} for $W(CH)(PH_3)_4Cl$) simplifies the description of the molecular orbitals relative to those of the C_2 symmetry dmpe complexes. It should be noted that the calculated molecular structures of $W(CH)(dmpe)_2Cl$ and $Cl(dmpe)_2WCCW(dmpe)_2Cl$ exhibit bond distances and angles very similar to those observed in the crystal structures of the compounds.[36] For $Cl(dmpe)_2WCCW(dmpe)_2Cl$, the calculated torsion angle between the two $W(dmpe)_2$ units is ca. 39° (relative to the pseudo D_{2h} symmetry conformer), which is consistent with the angle of ca. 45° observed in the (disordered) crystal structure.

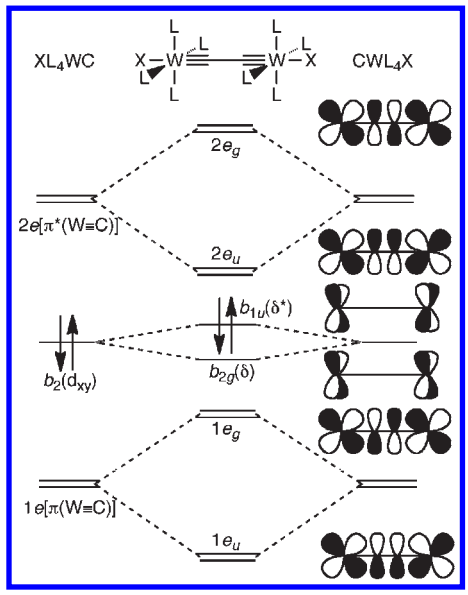

Figure 4. Qualitative molecular-orbital diagram of d^2-d^2 XL_4WCCWL_4X (D_{4h} symmetry).

The qualitative frontier molecular-orbital diagram of a D_{4h}-symmetry XL_4WCCWL_4X complex, shown in Figure 4, can be derived by mixing the frontier orbitals of two C_{4v}-symmetry $W(≡C)L_4Cl$ fragments. Prior experimental work[49−52] has established that for mononuclear d^2 complexes of the type $W(≡CR)L_4X$ (L = phosphine, X = halide, R = H or alkyl) the HOMO is a metal-centered d_{xy} orbital (b_2, Figure 4) that is nonbonding (δ symmetry) with respect to the X—W≡C axis and of π symmetry with respect to the equatorial L ligands. The LUMO (2*e*) is π*(W≡C) in character and comprised of $W(d_{xz},d_{yz})$ orbitals, and the HOMO−1 (1*e*) is the π(W≡C) bonding counterpart of the LUMO. In XL_4WCCWL_4X, the linear combinations of the monomer π(W≡C) orbitals form the levels $1e_u$ (π(W≡C—C≡W)) and $1e_g$ (π(W≡CC≡W)/π*(WC—CW)), which are π-bonding and antibonding, respectively, with respect to the C—C bond. The corresponding

(48) There is a prior report of an electronic-structure calculation of $W(CH)(PH_3)_4Cl$ (Vyboishchikov, S. F.; Frenking, G. *Chem.—Eur. J.* **1998**, *4*, 1439), but it does not report orbital energies.

(49) Bocarsly, A. B.; Cameron, R. E.; Rubin, H. D.; McDermott, G. A.; Wolff, C. R.; Mayr, A. *Inorg. Chem.* **1985**, *24*, 3976.
(50) Manna, J.; Gilbert, T. M.; Dallinger, R. F.; Geib, S. J.; Hopkins, M. D. *J. Am. Chem. Soc.* **1992**, *114*, 5870.
(51) van der Eide, E. F.; Piers, W. E.; Parvez, M.; McDonald, R. *Inorg. Chem.* **2007**, *46*, 14.
(52) Da Re, R. E.; Hopkins, M. D. *Coord. Chem. Rev.* **2005**, *249*, 1396.

combinations of the monomer π^*(W≡C) orbitals form the $2e_u$ orbital, which is π^*(W≡CC≡W)/π(WC—CW) in character, and all-antibonding $2e_g$ (π^*(W≡C—C≡W)). The forms of these orbitals are independent of the canonical structure of the backbone: they are also relevant to M—C≡C—M and M=C=C=M structures and are evident in calculations on compounds containing these motifs.[20,53,54] In addition to the π system orbitals, the monomer d_{xy} orbitals will combine to form $\delta(W_2)$ (b_{2g}) and $\delta^*(W_2)$ (b_{1u}) levels analogous to those of multiply metal−metal bonded dimers;[55] these should be split only slightly in energy due to the long W···W distance (5.1 Å, Table 2). The LUMO of an XL_4WCCWL_4X complex is expected to be $2e_u$, and the HOMO could be either b_{1u} $\delta^*(W_2)$ or $1e_g$, depending on the nature of L.

These qualitative bonding features are evident in the results of density-functional calculations on C_{4v}-symmetry W(CH)$(PH_3)_4$Cl (representing the W(C)$(PH_3)_4$Cl fragment) and D_{4h}-symmetry Cl$(PH_3)_4$WCCW$(PH_3)_4$Cl. The calculated frontier-orbital energies and Kohn−Sham orbitals are shown in Figures 5 and 6, respectively, and the atomic contributions to the orbitals are set out in Table 3. The LUMO, HOMO, and HOMO−1 of the two model compounds correspond to the qualitative orbitals depicted in Figure 4 and are 55−75% W or WC in character (Table 3). For W(CH)$(PH_3)_4$Cl, the HOMO is the d_{xy} orbital ($55b_2$); as expected from simple symmetry considerations, the d_{xy}-derived levels for Cl$(PH_3)_4$WCCW$(PH_3)_4$Cl ($107b_{1u}$ $\delta^*(W_2)$ and $106b_{2g}$ $\delta(W_2)$) lie at virtually the same energy as $55b_2$ and exhibit a δ/δ^* splitting of only 0.02 eV. The π(W≡C) orbital of W(CH)$(PH_3)_4$Cl (53/54e, HOMO−1) and the π(W≡CC≡W)/π^*(WC—CW) orbital of Cl$(PH_3)_4$WCCW$(PH_3)_4$Cl (108/109e_g, HOMO) contain appreciable contributions from the trans chloride ligands (35 and 17%, respectively) due to the close energetic proximity of the zero-order π(WC) levels to the chloride $3p_x$,p_y orbitals; each is π(WCl) in character. (The corresponding combinations with π(WCl) character lie to lower energy and are more chloride-localized.) The LUMOs of the compounds—π^*(WC) (56/57e) for W(CH)$(PH_3)_4$Cl and π^*(W≡CC≡W)/π(WC—CW) (110/111e_u) for Cl$(PH_3)_4$WCCW$(PH_3)_4$Cl—possess much smaller chloride contributions due to energy factoring of the parent orbitals. For Cl$(PH_3)_4$WCCW$(PH_3)_4$Cl, the π(W≡CC≡W)/π^*(WC—CW), $\delta^*(W_2)$, and $\delta(W_2)$ orbitals (106−109) lie within 0.1 eV of each other.

Because the compounds Cl$(dmpe)_2$WCCW$(dmpe)_2$Cl and Cl{P$(OMe)_3$}$_4$WCCW{P$(OMe)_3$}$_4$Cl exhibit noneclipsed conformations, calculations were performed on the model complex Cl$(PH_3)_4$WCCW$(PH_3)_4$Cl in the staggered (D_{4d} symmetry) geometry.[36] Given the cylindrical symmetry of the π-symmetry WCCW orbitals, it is unsurprising that their frontier orbital energies are unchanged (ΔE < 0.01 eV) from those of the D_{4h} rotamer. The principal difference between the orbitals of the two conformations is that the slightly split $\delta^*(W_2)$ and $\delta(W_2)$ orbitals found for D_{4h} collapse to degenerate (e_2 symmetry) d_{xy} orbitals, as expected from the fact that δ orbital overlap varies as cos 2θ (θ = torsion angle). The calculated difference in total energy between the D_{4h} and D_{4d} conformers is ca. 0.1 kcal mol^{-1}.

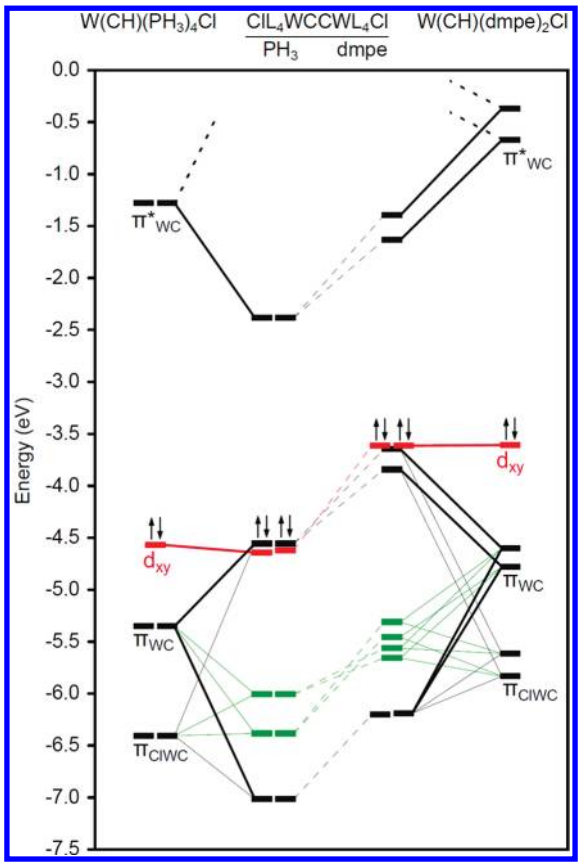

Figure 5. Calculated orbital energies for W(CH)$(PH_3)_4$Cl, Cl$(PH_3)_4$WCCW$(PH_3)_4$Cl, W(CH)$(dmpe)_2$Cl, and Cl$(dmpe)_2$WCCW$(dmpe)_2$Cl. Energies and atomic parentages of black-colored levels (π,π^*) and red levels (d_{xy}) are provided in Table 3; levels in green are principally of Cl parentage.

The calculated orbitals of W(CH)$(dmpe)_2$Cl and Cl$(dmpe)_2$WCCW$(dmpe)_2$Cl are more complex than those of the PH_3-containing model complexes, but clear correspondences among the frontier orbitals are evident (Figure 5). Further, the atomic contributions to orbitals of a given type are very similar between the PH_3 and dmpe derivatives (Table 3). This suggests that the simplified framework provided by the model complexes is suitable for interpreting the physical properties of the dmpe compounds. One general difference between dmpe and PH_3 derivatives is that the unsymmetrical P—W—P bond angles of the dmpe complexes (ca. 80° and 100° within and between the dmpe ligands, respectively) impose maximal C_2 symmetry, lifting the degeneracy of the e-symmetry orbitals of the PH_3 analogs. For W(CH)$(dmpe)_2$Cl, these orbital splittings are calculated to be ca. 0.2−0.3 eV, which is comparable to that deduced from electronic-spectroscopic studies on d^2

(53) (a) Neithamer, D. R.; LaPointe, R. E.; Wheeler, R. A.; Richeson, D. S.; Van Duyne, G. D.; Wolczanski, P. T. *J. Am. Chem. Soc.* **1989**, *111*, 9056. (b) Heidrich, J.; Steimann, M.; Appel, M.; Beck, W.; Phillips, J. R.; Trogler, W. C. *Organometallics* **1990**, *9*, 1296. (c) Belanzoni, P.; Re, N.; Rosi, M.; Sgamellotti, A.; Floriani, C. *Organometallics* **1996**, *15*, 4264. (d) Belanzoni, P.; Re, N.; Sgamellotti, A.; Floriani, C. *J. Chem. Soc., Dalton Trans.* **1997**, 4773. (e) Ouddai, N.; Costuas, K.; Bencharif, M.; Saillard, J. Y.; Halet, J. F. *C. R. Chim.* **2004**, *8*, 1336.

(54) Bruce, M. I.; Costuas, K.; Ellis, B. G.; Halet, J. F.; Low, P. J.; Moubaraki, B.; Murray, K. S.; Ouddai, N.; Perkins, G. J.; Skelton, B. W.; White, A. H. *Organometallics* **2007**, *26*, 3735.

(55) *Multiple Bonds between Metal Atoms*; 3rd ed.; Cotton, F. A., Murillo, C. A., Walton, R. A., Eds.; Springer: New York, 2005.

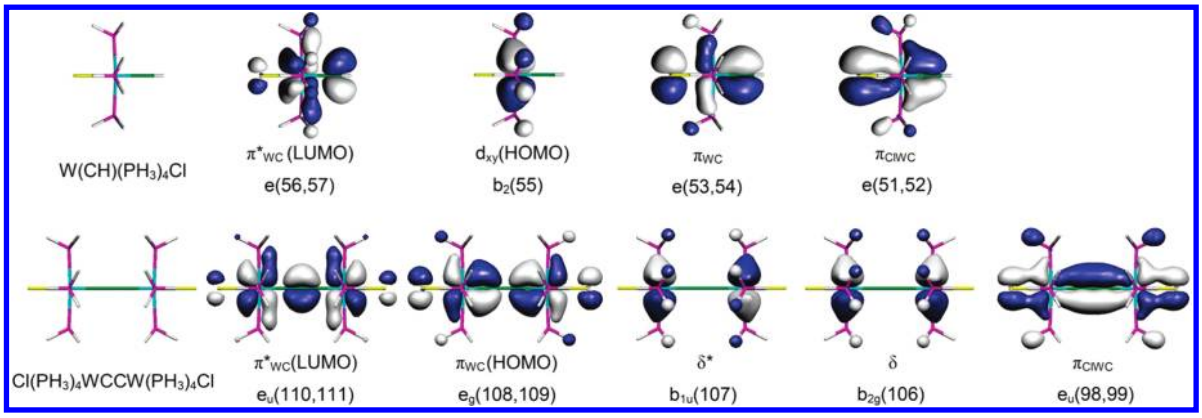

Figure 6. Selected Kohn−Sham orbitals for $W(CH)(PH_3)_4Cl$ and $Cl(PH_3)_4WCCW(PH_3)_4Cl$ (iso 0.97).

Table 3. Atomic Contributions to Selected Frontier Orbitals of $W(CH)L_4Cl$ and ClL_4WCCWL_4Cl[a]

			atomic parentage, %			
orbital	symmetry	energy (eV)	W	C	PR_3	Cl
		$W(CH)(PH_3)_4Cl$ (C_{4v})				
π^*_{WC} (LUMO)	56/57*e*	−1.28	38.2	32.7	25.8	3.3
d_{xy} (HOMO)	55b_2	−4.57	64.9	0.1	34.9	0.1
π_{WC}	53/54*e*	−5.35	23.8	31.4	9.6	35.3
π_{ClWC}	51/52*e*	−6.41	24.8	12.3	10.2	52.6
		$Cl(PH_3)_4WCCW(PH_3)_4Cl$ (D_{4h})				
π^*_{WC} (LUMO)	110/111e_u	−2.38	53.0	23.5	17.3	6.1
π_{WC} (HOMO)	108/109e_g	−4.56	53.2	16.9	12.8	17.1
δ^*	107b_{1u}	−4.62	65.3	0.1	34.6	0.1
δ	106b_{2g}	−4.64	64.5	0.1	35.2	0.1
π_{ClWC}	98/99e_u	−7.01	24.8	39.6	15.2	20.4
		$W(CH)(dmpe)_2Cl$ (C_2)[b]				
π^*_{WC}	105*b*	−0.37	57.2	28.5	12.0	2.3
π^*_{WC} (LUMO)	102*b*	−0.67	40.2	32.9	24.3	2.7
d_{xy} (HOMO)	101*a*	−3.61	66.4	0.3	33.3	0.0
π_{WC}	100*b*	−4.60	31.7	37.2	12.6	18.4
π_{WC}	99*b*	−4.78	30.2	33.4	12.7	23.7
π_{ClWC}	98*b*	−5.62	11.0	10.8	47.4	30.8
π_{ClWC}	97*b*	−5.83	16.0	11.5	28.9	43.6
		$Cl(dmpe)_2WCCW(dmpe)_2Cl$ (C_2)				
π^*_{WC}	203*b*	−1.40	55.3	22.5	18.8	3.5
π^*_{WC} (LUMO)	202*b*	−1.63	48.9	22.6	24.6	3.9
d_{xy} (HOMO)	201*a*	−3.61	65.6	0.3	34.1	0.0
d_{xy}	200*a*	−3.62	65.8	0.2	34.0	0.0
π_{WC}	199*b*	−3.65	61.4	19.7	11.2	7.8
π_{WC}	198*b*	−3.84	59.7	18.4	13.2	8.7
π_{C1WC}	192*b*	−6.19	14.8	18.1	32.2	34.8
π_{C1WC}	191*b*	−6.20	20.5	52.1	11.6	15.7

[a] Orbitals are depicted in Figures 5 and 6. [b] The structure of W(CH)(dmpe)$_2$Cl conforms closely to C_{2v} symmetry if the CH_n groups of the dmpe ligands are ignored; under the C_{2v} coordinate system, the d_{xy} and $d_{x^2-y^2}$ orbitals exchange designations (Da Re, R. E.; Hopkins, M. D. *Inorg. Chem.* **2002**, *41*, 6973).

$[Mo(O)(dmpe)_2Cl]^+$.[56] These splittings carry over to most of the π-type orbitals of $Cl(dmpe)_2WCCW(dmpe)_2Cl$. A second general observation is that orbital energies for the dmpe derivatives are 0.5 to 1.0 eV higher than the corresponding levels in the PH_3 derivatives, in line with the relative donor strengths of the two ligands.[57] Third, for $Cl(dmpe)_2WCCW(dmpe)_2Cl$, there is a reordering of the four highest occupied orbitals (198−201) relative to $Cl(PH_3)_4WCCW(PH_3)_4Cl$, with the isoenergetic d_{xy} orbitals now lying slightly higher in energy than the $\pi(W{\equiv}CC{\equiv}W)/\pi^*(WC{-}CW)$ orbitals. These orbitals still lie in a narrow energy range (0.2 eV), such that ordering is dependent on the functional used in the calculation.

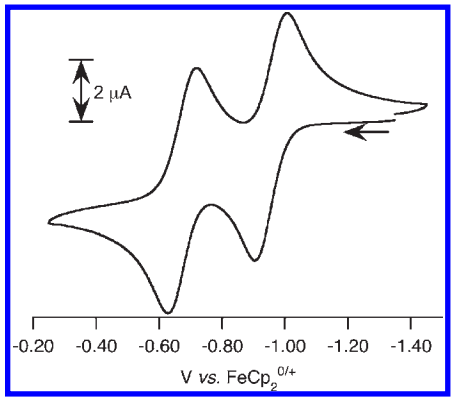

Figure 7. CV of $Cl(dmpe)_2WCCW(dmpe)_2Cl$ in THF/0.3 M $[NBu_4][PF_6]$, 0.100 V s^{-1}, 300 K.

Electrochemistry of d^2-d^2 ClL_4WCCWL_4Cl Complexes. The d^2-d^2 compounds of the form ClL_4WCCWL_4Cl exhibit two one-electron oxidations by cyclic voltammetry, which produce d^2-d^1 and d^1-d^1 redox congeners. A representative cyclic voltammogram (CV) of $Cl(dmpe)_2WCCW(dmpe)_2Cl$ in THF solution is shown in Figure 7; the CV of the compound in CH_2Cl_2 solution is qualitatively similar.[36] Two reversible oxidative waves are observed in THF at $E_{1/2}{}^{0/+} = -0.95$ V and $E_{1/2}{}^{+/2+} = -0.67$ V versus $FeCp_2{}^{0/+}$; these potentials shift to $E_{1/2}{}^{0/+} = -1.00$ V and $E_{1/2}{}^{+/2+} = -0.60$ V versus $FeCp_2{}^{0/+}$ in CH_2Cl_2. The potentials are independent of the scan rate (up to 1.00 V s^{-1}), and the waves exhibit $i_{pc}/i_{pa} \cong 1$, indicating that the processes are reversible. The separation between the peak potentials of the waves ($\Delta E_p = |E_{pc} - E_{pa}|$) for the 0/+ and +/2+ processes are in the ranges $\Delta E_p{}^{0/+} = 0.13-0.19$ V and $\Delta E_p{}^{+/2+} = 0.11-0.18$ V over these scan rates; under these conditions, $\Delta E_p{}^{0/+} = 0.11-0.15$ V for $FeCp_2$, supporting assignment of the waves to one-electron processes. The corresponding waves for $Cl\{P(OMe)_3\}_4WCCW\{P(OMe)_3\}_4Cl$ in THF are quasi-reversible (0/+) and irreversible (+/2+) even at

(56) Da Re, R. E.; Hopkins, M. D. *Inorg. Chem.* **2002**, *41*, 6973.
(57) Fey, N.; Orpen, A. G.; Harvey, J. N. *Coord. Chem. Rev.* **2009**, *253*, 704.

Table 4. Oxidation Potentials (V versus $FeCp_2^{0/+}$) of Tungsten−Alkylidyne Complexes[a]

compound	$E_{1/2}{}^{0/+}$	$E_{1/2}{}^{+/2+}$	solvent
$Cl(dmpe)_2WCCW(dmpe)_2Cl$	−0.95 (2)	−0.67 (1)	THF[b]
$W(CH)(dmpe)_2Cl$[51]	−0.91	n/a	THF[c]
$Cl(dmpe)_2WCCW(dmpe)_2Cl$	−1.00 (1)	−0.60 (1)	CH_2Cl_2[b]
$W(CPh)(dmpe)_2Cl$	−0.83 (1)	n/a	CH_2Cl_2[b]
$Cl\{P(OMe)_3\}_4WCCW\{P(OMe)_3\}_4Cl$	−0.26[d,e]	+0.22[f]	THF[b]
$W(CPh)\{P(OMe)_3\}_4Cl$[g]	−0.28[d,e]	n/a	THF[b]

[a] Measurements were conducted at room temperature unless otherwise noted. [b] Supporting electrolyte is $[NBu_4][PF_6]$ (0.3 M). [c] Supporting electrolyte is $[NBu_4][PF_6]$ (0.1 M). [d] Quasi-reversible. [e] Measurement performed at −13 °C. [f] Irreversible; approximate $E_{1/2}$ listed. [g] Haines, D. E., Ph. D. Thesis, The University of Chicago, 2001.

low temperatures (−13 °C) and fast scan rates and are centered at $E_{1/2}{}^{0/+} = -0.26$ V and $E^{+/2+} \cong +0.22$ V versus $FeCp_2^{0/+}$. Electrochemical data for these and related mononuclear tungsten−alkylidyne compounds are collected in Table 4.

The two one-electron oxidations of the ClL_4WCCWL_4Cl complexes are assigned to the successive removal of electrons from the d_{xy} orbitals on each tungsten center, to give $(d_{xy})^2-(d_{xy})^1$ and $(d_{xy})^1-(d_{xy})^1$ configured ions. The assignment of the first oxidation is based on the molecular-orbital description of the compounds (vide supra), which indicates that the energies of the d_{xy}-derived orbitals of the dimers are nearly identical to that of the d_{xy} HOMO of mononuclear $W(CR)L_4Cl$ for a given L ligand. For $W(CR)(PR'_3)_4X$ compounds, the first oxidation has been assigned to removal of a d_{xy} electron on the basis of structural[50] and EPR[51] studies. Comparisons between the $E_{1/2}{}^{0/+}$ potentials for $Cl(dmpe)_2WCCW(dmpe)_2Cl$, $Cl\{P(OMe)_3\}_4WCCW\{P(OMe)_3\}_4Cl$, and corresponding monometallic tungsten−alkylidyne compounds (Table 4) show that they differ by only 0.02−0.13 V between mono- and dimetallic complexes with a given L (dmpe or $P(OMe)_3$), strongly suggesting that the redox-active orbital is of the same parentage for both. The increase in $E_{1/2}{}^{0/+}$ by 0.7 V for $Cl\{P(OMe)_3\}_4WCCW\{P(OMe)_3\}_4Cl$ relative to $Cl(dmpe)_2WCCW(dmpe)_2Cl$ is consistent with the greater π-backbonding ability of $P(OMe)_3$, which stabilizes the d_{xy} orbitals.

The assignment of the second oxidation to $(d_{xy})^2-(d_{xy})^1 \rightarrow (d_{xy})^1-(d_{xy})^1$ is less straightforward. The separation between the first and second oxidation potentials, $\Delta E_{1/2} = |E_{1/2}{}^{0/+} - E_{1/2}{}^{+/2+}|$, is 0.28 V (THF) and 0.40 V (CH_2Cl_2) for $Cl(dmpe)_2WCCW(dmpe)_2Cl$, and ca. 0.5 V for $Cl\{P(OMe)_3\}_4WCCW\{P(OMe)_3\}_4Cl$ (THF).[58] The electronic-structure calculations for $Cl(dmpe)_2WCCW(dmpe)_2Cl$ indicate that the d_{xy}-derived orbitals (200/201, HOMO and HOMO−1) are split by ca. 0.01 eV, and that the upper bound on the $\delta/\delta^*(W_2)$ splitting for an eclipsed conformation (i.e., D_{4h} $Cl(PH_3)_4WCCW(PH_3)_4Cl$) is 0.02 eV. The fact that these orbital splittings are more than an order of magnitude smaller than $\Delta E_{1/2}$ does not straightforwardly support assignment of the second oxidation to removal of an electron from the second d_{xy} orbital. Alternatively, the second oxidation could be assigned to removal of an electron from a $\pi(W{\equiv}CC{\equiv}W)/\pi^*(WC{-}CW)$ orbital (Figure 5), which are calculated to lie ca. 0.2 eV lower than the d_{xy} levels (198/199, Table 3). However, this assignment is not intuitively consistent with the electrochemical reversibility observed for $Cl(dmpe)_2WCCW(dmpe)_2Cl$ because the resulting π-radical is unlikely to be stable. For example, the d^0-d^0 compound $(Bu^tO)_3WCCW(OBu^t)_3$ exhibits two irreversible oxidations (E_p = −0.354 and 0.100 V versus $FeCp_2^{0/+}$), at least the first of which is likely associated with the removal of electrons from the $\pi(W{\equiv}CC{\equiv}W)/\pi^*(WC{-}CW)$ HOMO of that compound.[20]

It is proposed that the shift of the second d_{xy}-based oxidation to a potential more positive than expected from molecular-orbital considerations is principally electrostatic in origin. For the equilibrium

$$ClL_4WCCWL_4Cl + [ClL_4WCCWL_4Cl]^{2+} = 2[ClL_4WCCWL_4Cl]^{+}$$

the comproportionation constant is given by $K_{com} = [WCCW^+]^2/[WCCW][WCCW^{2+}] = \exp[(\Delta E_{1/2})F/RT]$.[59] In the limit of identical, noninteracting redox orbitals, $K_{com} = 4$, corresponding to $\Delta E_{1/2} = 0.036$ V.[60] Estimating the Coulombic repulsion between the two tungsten centers with a simple dielectric continuum model and ignoring orbital overlap, antiferromagnetic exchange,[61] and inductive contributions to the equilibrium provides[62]

$$\Delta E_{1/2} = 1/(4\pi\varepsilon\varepsilon_o R_{ij}) + 0.036V$$

where ε is the dielectric constant of the medium, ε_o is the vacuum permittivity constant, and R_{ij} is the distance between the two metal centers. We are unaware of reports of the dielectric constants of CH_2Cl_2 and THF solutions of $[NBu_4][PF_6]$, but there are data for these solvents with $[NBu_4][BF_4]$[63] and $[NBu_4][ClO_4]$[64] that can be extrapolated to the electrolyte concentration (0.3 M) used in this study ($CH_2Cl_2/[NBu_4][BF_4]$, $\varepsilon = 21$; $CH_2Cl_2/[NBu_4][ClO_4]$, $\varepsilon = 13$; and $THF/[NBu_4][ClO_4]$, $\varepsilon = 12$) These values are likely to underestimate $\Delta E_{1/2}$ for the electrolyte $[NBu_4][PF_6]$; a detailed study by Geiger and Barriere of the dependence on the nature of the electrolyte of the redox potentials of a mixed-valence ferrocenyl-containing derivative demonstrated that $\Delta E_{1/2}$ was larger with $[NBu_4][PF_6]$ as the electrolyte in THF and CH_2Cl_2 than for $[NBu_4][ClO_4]$ and $[NBu_4][BF_4]$.[65] Despite these approximations and the simplicity of the model, the calculated "electrostatic only" values of $\Delta E_{1/2}(CH_2Cl_2) = 0.18-0.26$ V and $\Delta E_{1/2}(THF) = 0.28$ V are in reasonable agreement with the observed splittings for $Cl(dmpe)_2WCCW(dmpe)_2Cl$ of $\Delta E_{1/2}(CH_2Cl_2) = 0.40$ V and $\Delta E_{1/2}(THF) = 0.28$ V, supporting assignment

(58) For $Cl\{P(OMe)_3\}_4WCCW\{P(OMe)_3\}_4Cl$, the 0/+ couple is quasi-reversible and the +/2+ couple is irreversible, so $\Delta E_{1/2}$ and K_{com} are not well defined.

(59) Richardson, D. E.; Taube, H. *Inorg. Chem.* **1981**, *20*, 1278.
(60) Ammar, F.; Saveant, J. M. *J. Electroanal. Chem.* **1973**, *47*, 215.
(61) The antiferromagnetic coupling in d^1-d^1 $[Cl(depe)_2WCC_6H_4\text{-}4\text{-}CW(depe)_2Cl]^{2+}$ has been determined to be $J < 0.005$ eV (Hu, J. S.; Sun, J.; Hopkins, M. D.; Rosenbaum, T. F. *J. Phys.: Condens. Matter* **2006**, *18*, 10837). The W···W distance in this ion is 9.4 Å.
(62) Ferrere, S.; Elliott, C. M. *Inorg. Chem.* **1995**, *34*, 5818.
(63) Bao, D. D.; Millare, B.; Xia, W.; Steyer, B. G.; Gerasimenko, A. A.; Ferreira, A.; Contreras, A.; Vullev, V. I. *J. Phys. Chem. A* **2009**, *113*, 1259.
(64) Sigvartsen, T.; Gestblom, B.; Noreland, E.; Songstad, J. *Acta Chem. Scand.* **1989**, *43*, 103.
(65) Barriere, F.; Geiger, W. E. *J. Am. Chem. Soc.* **2006**, *128*, 3980.

Table 5. Electrochemical Data for Selected $L_nM(CC)_mML_n$ Complexes[a]

compound	$\Delta E_{1/2}$, V	K_{com}	d(MM), Å	redox orbital symmetry	ref
$Cl(dmpe)_2W{\equiv}C{-}C{\equiv}W(dmpe)_2Cl$	0.40	6×10^6	5.1	δ	
$[Cp'(dmpe)Mn{\equiv}C{-}C{\equiv}Mn(dmpe)Cp']^{2+}$	0.99	9×10^{16}	4.8	π	22
$Cp(dppe)Ru{-}C{\equiv}C{-}Ru(dppe)Cp$	0.82	7×10^{13}	5.3	π	54
$Tp'(CO)_2W{\equiv}CC{\equiv}CC{\equiv}W(CO)_2Tp'$	0.28	5×10^4	ca. 8[b]	δ	21
$Cp^*(dppe)Fe(C{\equiv}C)_2Fe(dppe)Cp^*$	0.73	2×10^{12}	7.6	π	66, 67
$Cp^*(PPh_3)(NO)Re(C{\equiv}C)_2Re(NO)(PPh_3)Cp^*$	0.53	1×10^9	7.8	π	68
$Cp^*(dppe)Fe(C{\equiv}C)_4Fe(dppe)Cp^*$	0.43	2×10^7	ca. 13[b]	π	4
$Cp^*(PPh_3)(NO)Re(C{\equiv}C)_6Re(NO)(PPh_3)Cp^*$	0.19	2×10^3	ca. 18[b]	π	9

[a] All data were obtained in CH_2Cl_2/0.1 M $[NBu_4][PF_6]$ except for $Cl(dmpe)_2WCCW(dmpe)_2Cl$ (CH_2Cl_2/0.3 M $[NBu_4][PF_6]$), $Cp^*(PPh_3)(NO)Re(C{\equiv}C)_2Re(NO)(PPh_3)Cp^*$ (CH_2Cl_2/0.1 M $[NBu_4][BF_4]$), and $[Cp'(dmpe)Mn{\equiv}C{-}C{\equiv}Mn(dmpe)Cp']^{2+}$ (CH_3CN/0.1 M $[NBu_4][PF_6]$). [b] Crystallographic data not available; distance estimated from standard bond lengths.

of the second oxidation to removal of a d_{xy} electron and suggesting that nonelectrostatic contributions to $\Delta E_{1/2}$ are small.

Further context for the weak interaction between the redox orbitals of XL_4WCCWL_4X compounds can be gleaned by comparing the magnitude of K_{com} to those for $L_nM(CC)_mML_n$ complexes for which the redox orbitals are conjugated with the π backbone. For $Cl(dmpe)_2WCCW(dmpe)_2Cl$, the values of $\Delta E_{1/2}$ correspond to $K_{com} = 5 \times 10^4$ (THF) and 6×10^6 (CH_2Cl_2). These data, and selected data for other $L_nM(CC)_mML_n$ complexes, are set out in Table 5. Because of the solvent/electrolyte dependence of $\Delta E_{1/2}$ (and, hence, K_{com}),[65] it is prudent to restrict comparisons to data measured in identical (or closely similar) electrochemical media; in the present case, the solvent most commonly used in prior studies is CH_2Cl_2. From an electronic-structure standpoint, the compound in Table 5 most closely related to the present systems is $Tp'(CO)_2W{\equiv}CC{\equiv}CC{\equiv}W(CO)_2Tp'$, for which a similar $(d_{xy})^2{-}(d_{xy})^2$ ground-state electron configuration was proposed on the basis of an extended-Hückel calculation.[21] For this compound, $K_{com} = 5 \times 10^4$ in CH_2Cl_2; the 100-fold decrease of K_{com} relative to that for $Cl(dmpe)_2WCCW(dmpe)_2Cl$ ($K_{com} = 6 \times 10^6$ in CH_2Cl_2) is reasonable, given the increase in W···W distance from 5.1 to ca. 7.7 Å. In contrast to these δ-symmetry systems, $L_nM(CC)_mML_n$ compounds whose redox orbitals are of π or π^* symmetry with respect to the $M(CC)_mM$ backbone exhibit much larger values of K_{com} at comparable metal−metal distances. For example, the values of K_{com} for the C_2-bridged compounds $Cp(dppe)Ru{-}C{\equiv}C{-}Ru(dppe)_2Cp$ (7×10^{13})[54] and $[Cp'(dmpe)Mn{\equiv}C{-}C{\equiv}Mn(dmpe)Cp']^{2+}$ (9×10^{16}, in CH_3CN)[22] exceed that of $Cl(dmpe)_2WCCW(dmpe)_2Cl$ by $>10^7$ fold despite their similar M···M distances. For longer $L_nM(CC)_mML_n$ compounds with π/π^* symmetry redox orbitals, K_{com} does not approach 10^6 until $m = 4$, corresponding to metal−metal distances of ≥13 Å. As noted by Thorp, Templeton, and co-workers in their study of $Tp'(CO)_2W{\equiv}CC{\equiv}CC{\equiv}W(CO)_2Tp'$,[21] the relatively small value of K_{com} for the $(d_{xy})^2{-}(d_{xy})^2$ configuration does not imply that the backbone is weakly π conjugated but rather is the result of the orthogonality between the δ-symmetry redox orbitals and the π-conjugated backbone. As a consequence of this orthogonality, the $(d_{xy})^2{-}(d_{xy})^2$, $(d_{xy})^2{-}(d_{xy})^1$, and $(d_{xy})^1{-}(d_{xy})^1$ redox congeners of $Cl(dmpe)_2WCCW(dmpe)_2Cl$ all possess formal $W{\equiv}C{-}C{\equiv}W$ canonical structures; in contrast, the redox reactions of $L_nM(CC)_mML_n$ compounds with π-symmetry redox orbitals change MC and CC bond orders.

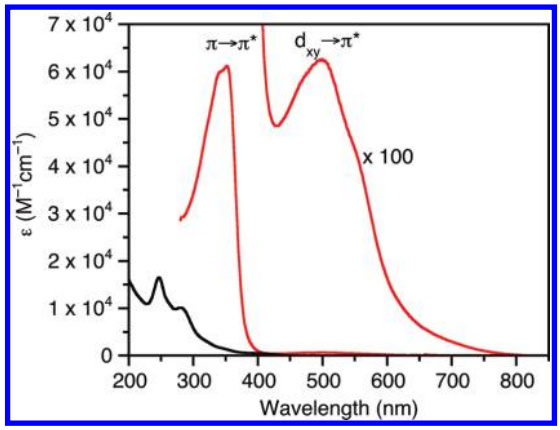

Figure 8. Electronic-absorption spectrum of $Cl(dmpe)_2WCCW(dmpe)_2Cl$ (red) in toluene and $W(CH)(dmpe)_2Cl$ (black) in 2-methylpentane at room temperature.

Electronic-Absorption Spectroscopy. On the basis of molecular-orbital considerations for the model complex $Cl(PH_3)_4WCCW(PH_3)_4Cl$ (Figures 4 and 5), $d^2{-}d^2$ compounds of this general class are expected to exhibit bands attributable to electronic transitions of orbital character $\pi \rightarrow \pi^*$ ($1e_g \rightarrow 2e_u$, Figure 4) and $d_{xy}(\delta,\delta^*) \rightarrow \pi^*$ ($b_{2g} \rightarrow 2e_u$, $b_{1u} \rightarrow 2e_u$) as the lowest-energy features. Under D_{4h} symmetry, the dipole-allowed transitions are $\delta \rightarrow \pi^*$ ($A_{1g} \rightarrow E_u$) and $\pi \rightarrow \pi^*$ ($A_{1g} \rightarrow A_{2u}$), while $\delta^* \rightarrow \pi^*$ ($A_{1g} \rightarrow E_g$) and the $\pi \rightarrow \pi^*$ transitions that produce A_{1u}, B_{1g}, and B_{1u} excited states are dipole-forbidden. For $Cl(dmpe)_2WCCW(dmpe)_2Cl$, the degeneracy of the e-symmetry π and π^* orbitals is lifted by the chelating dmpe ligands (vide supra), producing up to four $d_{xy} \rightarrow \pi^*$ and four $\pi \rightarrow \pi^*$ bands; all will be dipole-allowed. For reference, prior studies have established that monometallic metal−alkylidyne complexes exhibit spin-allowed $d_{xy} \rightarrow \pi^*$ bands (ε 10^2 M^{-1} cm^{-1}) in the 400−600 nm region and $\pi \rightarrow \pi^*$ bands (ε 10^4 M^{-1} cm^{-1}) in the 300−400 nm region.[52] The relatively low intensity of the dipole-allowed $d_{xy} \rightarrow \pi^*$ band is due to the underlying $d \rightarrow d$ character of the transition.

The electronic-absorption spectrum of $Cl(dmpe)_2WCCW(dmpe)_2Cl$ in toluene, shown in Figure 8, exhibits

(66) Jiao, H. J.; Costuas, K.; Gladysz, J. A.; Halet, J. F.; Guillemot, M.; Toupet, L.; Paul, F.; Lapinte, C. *J. Am. Chem. Soc.* **2003**, *125*, 9511.
(67) Lenarvor, N.; Toupet, L.; Lapinte, C. *J. Am. Chem. Soc.* **1995**, *117*, 7129.
(68) Brady, M.; Weng, W. Q.; Zhou, Y. L.; Seyler, J. W.; Amoroso, A. J.; Arif, A. M.; Bohme, M.; Frenking, G.; Gladysz, J. A. *J. Am. Chem. Soc.* **1997**, *119*, 775.

bands consistent with these expectations. Two prominent bands are observed: a broad, multicomponent band at λ_{max} = 500 nm (ε 630 M^{-1} cm^{-1}) assigned to $^1(d_{xy} \rightarrow \pi^*)$ and an intense band at λ_{max} = 352 nm (ε 61 200 M^{-1} cm^{-1}) assigned to $^1(\pi \rightarrow \pi^*)$. The breadth of the $d_{xy} \rightarrow \pi^*$ band presumably arises from two (or more) closely spaced transitions to the nondegenerate π^* levels (Figure 5). The $\pi \rightarrow \pi^*$ band exhibits a vibronic shoulder at 340 nm, corresponding to a frequency of ca. 1000 cm^{-1}. Given that the transition produces an excited state that weakens the WC bonds and strengthens the CC bond, it is logical to assign this feature to an excited-state WCCW stretching mode. For reference, the W≡CR mode of monometallic tungsten−alkylidyne complexes is observed at frequencies of 1275−1400 cm^{-1} (R ≠ H),[69] and the C−C stretch of butadiyne is observed at 874 cm^{-1}.[70] It is probable that these oscillators will be strongly coupled in the present compounds, precluding assignment of the vibronic frequency to a localized coordinate.

The absorption spectra of Cl{P(OMe)$_3$}$_4$WCCW{P(OMe)$_3$}$_4$Cl and (TfO)(dmpe)$_2$WCCW(dmpe)$_2$(OTf)[36] in toluene are qualitatively similar to that for Cl(dmpe)$_2$WCCW(dmpe)$_2$Cl, displaying $^1(d_{xy} \rightarrow \pi^*)$ bands at 460 and 515 nm and $^1(\pi \rightarrow \pi^*)$ bands at 335 and 321 nm, respectively. The spectrum of d^0-d^0 [Cl(dmpe)$_2$(H)WCCW(H)(dmpe)$_2$Cl]$^{2+}$ lacks the $^1(d_{xy} \rightarrow \pi^*)$ band, because the d_{xy} electrons are involved in the W−H bonds, but displays the $^1(\pi \rightarrow \pi^*)$ band at 324 nm in CH_2Cl_2.[36] The fact that the $^1(\pi \rightarrow \pi^*)$ transition energy is observed across a relatively narrow range (2600 cm^{-1}) as the equatorial and axial ligands and metal oxidation state is varied supports the conclusion from the calculations that the π and π^* orbitals are largely WCCW-localized in character.

The relationship between these electronic transition energies and those of analogous monometallic metal−alkylidyne compounds and of organic polyynes demonstrates the presence of substantial W≡CC≡W π conjugation and the strong contribution to it of the metal d orbitals. The electronic-absorption spectrum of W(CH)(dmpe)$_2$Cl, the closest monomer analog of Cl(dmpe)$_2$WCCW(dmpe)$_2$Cl, is displayed in Figure 8. Unlike the ditungsten compound, W(CH)(dmpe)$_2$Cl is soluble in alkane solvents, allowing characterization of the spectrum deeper into the UV region; the $^1(d_{xy} \rightarrow \pi^*)$ band is observed at 403 nm (ε 500 M^{-1} cm^{-1})[46] and the $^1(\pi \rightarrow \pi^*)$ band at 280 nm (ε 10 100 M^{-1} cm^{-1}), while the band at 247 nm (ε 16 500 M^{-1} cm^{-1}) is tentatively assigned to the $^1(\pi(ClWC) \rightarrow \pi^*)$ transition. The substantial red shifts of the $^1(d_{xy} \rightarrow \pi^*)$ and $^1(\pi \rightarrow \pi^*)$ bands of Cl(dmpe)$_2$WCCW(dmpe)$_2$Cl compared to those of W(CH)(dmpe)$_2$Cl, by ca. 0.6 and 0.9 eV, respectively, are consistent with the strong W≡CC≡W π conjugation evidenced in the electronic-structure calculations. Also of note is the substantial red shift of the $^1(\pi \rightarrow \pi^*)$ band of the d^0-d^0 and d^2-d^2 compounds relative to organic polyynes. For $Pr^i_3SiC{\equiv}CC{\equiv}CSiPr^i_3$, an organic analog of the present compounds, the $^1(\pi \rightarrow \pi^*)$ band is observed at λ_{max} < 210 nm—a blue shift of >2.3 eV relative to Cl(dmpe)$_2$WCCW(dmpe)$_2$Cl—and it is only for $Pr^i_3Si(C{\equiv}C)_nSiPr^i_3$ oligomers of length $n \cong 8-10$ that the $^1(\pi \rightarrow \pi^*)$ band maximum approaches that for Cl(dmpe)$_2$WCCW(dmpe)$_2$Cl.[71] The strong red shift of the $^1(\pi \rightarrow \pi^*)$ band for the WCCW compounds from that of organic analogs demonstrates the strong participation of the d orbitals in the W≡CC≡W π conjugation and suggests the strong control over π bandgaps that might be achieved in metal-containing polyynes of type **I** (Chart 1).

Conclusions

We have found that the synthesis of d^2-d^2 compounds of the type XL$_4$WCCWL$_4$X (L = 1/2 dmpe, 1/2 depe, P(OMe)$_3$; X = Cl, OTf) can be accomplished in two steps and moderate yield from readily available (Bu^{t}O)$_3$WCCW(OBu^t)$_3$. The molecular structures of these compounds are consistent with a W≡C—C≡W canonical structure within the backbone. Comparisons between the calculated electronic structures and the electronic spectra of XL$_4$WCCWL$_4$X and analogous monometallic W(CH)L$_4$X compounds indicate that the WCCW backbone is characterized by strong π conjugation, and that the HOMO and HOMO−1 of XL$_4$WCCWL$_4$X are axially nonbonding (δ symmetry) metal-centered levels. These latter orbitals endow the compounds with rich redox chemistry: d^2-d^1 and d^1-d^1 congeners are accessible via electrochemical oxidation, and the d^0-d^0 hydride derivative [Cl(H)(dmpe)$_2$WCCW(dmpe)$_2$(H)Cl]$^{2+}$ may be synthesized via protonation. Importantly, these redox transformations leave intact the W≡C—C≡W canonical structure. This family of compounds expands the relatively small class of M≡C—C≡M complexes and affords the opportunity to construct type **I** materials that should possess broad redox properties while retaining the alternating-bond-order structures of parent carbyne. Work directed toward the preparation of such materials will be reported separately.

Acknowledgment. We are grateful to Jason Sonnenberg and Prof. Bruce Bursten for performing preliminary DFT calculations, and to Dr. Ian Steele for providing the X-ray crystallographic data. This research was supported through the NSF MRSEC Program, Grant DMR-0820054, and by the University of Chicago−Argonne National Laboratory Joint Theory Institute.

Supporting Information Available: X-ray crystallographic data for Cl(dmpe)$_2$WCCW(dmpe)$_2$Cl, Cl{P(OMe)$_3$}$_4$WCCW{P(OMe)$_3$}$_4$Cl, and [Cl(H)(dmpe)$_2$WCCW(dmpe)$_2$(H)Cl]Cl$_2$ in CIF format; atomic coordinates, selected bond distances, and orbital energies and atomic parentages from density-functional theory calculations of W(CH)(dmpe)$_2$Cl, W(CH)(PH$_3$)$_4$Cl, Cl(dmpe)$_2$WCCW(dmpe)$_2$Cl, and Cl(PH$_3$)$_4$WCCW(PH$_3$)$_4$Cl; cyclic voltammogram of Cl(dmpe)$_2$WCCW(dmpe)$_2$Cl in CH_2Cl_2; and electronic spectra of (TfO)(dmpe)$_2$WCCW(dmpe)$_2$(OTf) and [Cl(H)(dmpe)$_2$WCCW(dmpe)$_2$(H)Cl]Cl$_2$. This material is available free of charge via the Internet at http://pubs.acs.org.

(69) (a) Dao, N. Q. *J. Organomet. Chem.* **2003**, *684*, 82. (b) Manna, J.; Dallinger, R. F.; Miskowski, V. M.; Hopkins, M. D. *J. Phys. Chem. B* **2000**, *104*, 10928. (c) Manna, J.; Kuk, R. J.; Dallinger, R. F.; Hopkins, M. D. *J. Am. Chem. Soc.* **1994**, *116*, 9793.

(70) Chang, K. W.; Graham, W. R. M. *J. Mol. Spectrosc.* **1982**, *94*, 69.

(71) Eisler, S.; Slepkov, A. D.; Elliott, E.; Luu, T.; McDonald, R.; Hegmann, F. A.; Tykwinski, R. R. *J. Am. Chem. Soc.* **2005**, *127*, 2666.